Conformational states of syntaxin-1 govern the necessity of N-peptide binding in exocytosis of PC12 cells and *Caenorhabditis elegans*

Seungmee Park[a,b], Na-Ryum Bin[a,b], Maaran Michael Rajah[a], Byungjin Kim[a], Ting-Chieh Chou[a,b], Soo-young Ann Kang[a], Kyoko Sugita[c], Leon Parsaud[a,b], Matthew Smith[d,e], Philippe P. Monnier[b,c], Mitsuhiko Ikura[c,d], Mei Zhen[f,g], and Shuzo Sugita[a,b,*]

[a]Division of Fundamental Neurobiology and [c]Division of Genetics and Development, Krembil Discovery Tower, University Health Network, Toronto, ON M5T 2S8, Canada; [b]Department of Physiology and [g]Department of Molecular Genetics, University of Toronto, Toronto, ON M5S 1A8, Canada; [d]Division of Signaling Biology, MaRS Toronto Medical Discovery Tower, Ontario Cancer Institute, University Health Network, Toronto, ON M5G 1L7, Canada; [e]Department of Medical Biophysics, University of Toronto, Toronto, ON M5G 1L7, Canada; [f]Lunenfeld-Tanenbaum Research Institute, Mount Sinai Hospital, Toronto, ON M5G 1X5, Canada

ABSTRACT **Syntaxin-1 is the central SNARE protein for neuronal exocytosis. It interacts with Munc18-1 through its cytoplasmic domains, including the N-terminal peptide (N-peptide). Here we examine the role of the N-peptide binding in two conformational states ("closed" vs. "open") of syntaxin-1 using PC12 cells and *Caenorhabditis elegans*. We show that expression of "closed" syntaxin-1A carrying N-terminal single point mutations (D3R, L8A) that perturb interaction with the hydrophobic pocket of Munc18-1 rescues impaired secretion in syntaxin-1–depleted PC12 cells and the lethality and lethargy of *unc-64* (*C. elegans* orthologue of syntaxin-1)-null mutants. Conversely, expression of the "open" syntaxin-1A harboring the same mutations fails to rescue the impairments. Biochemically, the L8A mutation alone slightly weakens the binding between "closed" syntaxin-1A and Munc18-1, whereas the same mutation in the "open" syntaxin-1A disrupts it. Our results reveal a striking interplay between the syntaxin-1 N-peptide and the conformational state of the protein. We propose that the N-peptide plays a critical role in intracellular trafficking of syntaxin-1, which is dependent on the conformational state of this protein. Surprisingly, however, the N-peptide binding mode seems dispensable for SNARE-mediated exocytosis per se, as long as the protein is trafficked to the plasma membrane.**

Monitoring Editor
Benjamin S. Glick
University of Chicago

Received: Sep 8, 2015
Revised: Dec 12, 2015
Accepted: Dec 18, 2015

INTRODUCTION

The soluble *N*-ethylmaleimide–sensitive factor attachment protein receptor (SNARE) complex composed of syntaxin-1, SNAP-25, and synaptobrevin (VAMP2) is believed to play central roles in the fusion of secretory vesicles with the plasma membrane in the final step of neuronal exocytosis (Söllner *et al.*, 1993; Jahn, 2004; Südhof and Rothman, 2009). This hypothesis has been genetically supported by the analysis of many mutants lacking the SNARE proteins in various organisms, including mice, *Drosophila,* and *Caenorhabditis elegans* (Broadie *et al.*, 1995; Schulze *et al.*, 1995; Nonet *et al.*, 1998; Saifee *et al.*, 1998; Schoch *et al.*, 2001; Washbourne *et al.*, 2002). For instance, the lack of syntaxin-1 caused complete loss of both evoked and spontaneous neurotransmitter release in *Drosophila* (Schulze *et al.*, 1995) and almost complete paralysis in *C. elegans* (Saifee *et al.*, 1998; Richmond *et al.*, 2001).

In mammals, syntaxin-1A and 1B, two closely related isoforms of syntaxin-1, are predominantly expressed in the nervous system (Bennett *et al.*, 1992). Syntaxin-1A–deficient mice exhibited normal basic neurotransmission even though monoaminergic transmission and long-term potentiation were partially impaired (Fujiwara *et al.*, 2006; Mishima *et al.*, 2012). In contrast, loss of

This article was published online ahead of print in MBoC in Press (http://www.molbiolcell.org/cgi/doi/10.1091/mbc.E15-09-0638) on December 23, 2015.
The authors declare no conflict of interest.
*Address correspondence to: Shuzo Sugita (ssugita@uhnres.utoronto.ca).
Abbreviations used: GST, glutathione *S*-transferase; ITC, isothermal titration calorimetry; NA, noradrenalin; PC12, pheochromocytoma 12; SNARE, *N*-ethylmaleimide–sensitive factor attachment protein receptor.

Supplemental Material can be found at:
http://www.molbiolcell.org/content/suppl/2015/12/21/mbc.E15-09-0638v1.DC1.html

syntaxin-1B alone caused mice to die within 2 wk after birth (Kofuji *et al.*, 2014; Mishima *et al.*, 2014). Mice lacking both isoforms suffered from embryonic lethality (Mishima *et al.*, 2014), which suggests a partial functional redundancy between the two isoforms. Many neurons derived from the double-knockout fetuses degenerated in culture (Mishima *et al.*, 2014). Few neurons that were able to survive exhibited significantly reduced spontaneous events and highly asynchronous evoked response (Mishima *et al.*, 2014). These results demonstrate that syntaxin-1 is necessary for neuronal survival, synaptic transmission, and the viability of mice.

One of the binding partners of syntaxins is Munc18-1, which is an essential regulator of neuronal SNARE-mediated membrane fusion/exocytosis (Han *et al.*, 2010). Munc18-1 and its orthologues are required for neurotransmitter release, as demonstrated in genetic studies of several model organisms (Hosono *et al.*, 1992; Harrison *et al.*, 1994; Verhage *et al.*, 2000; Weimer *et al.*, 2003). Munc18-1 has two different modes of binding to syntaxin-1 (Burgoyne and Morgan, 2007; Südhof and Rothman, 2009; Han *et al.*, 2010). In the first binding mode, Munc18-1 binds to the "closed" syntaxin-1 with high affinity through its cleft formed by domain-1 and 3a (Misura *et al.*, 2000). The second binding mode involves the binding between syntaxin-1 N-peptide and the outer surface of hydrophobic pocket of Munc18-1 (Burkhardt *et al.*, 2008). The interchange between the two binding modes and their contribution to exocytosis remain unclear.

The role of the latter binding mode has been a hot topic and highly debated in the field of exocytosis. Based on the liposome fusion assays, it has been hypothesized to play a critical role for Munc18-mediated, SNARE-dependent membrane fusion (Supplemental Figure S1A; Shen *et al.*, 2007; Südhof and Rothman, 2009). Supporting this hypothesis, Zhou *et al.* (2013) demonstrated that deletion of N-peptide abolishes the ability of syntaxin-1A to rescue exocytosis in synatxin-1A–null, syntaxin-1B–knockdown neurons. This suggests an absolutely essential role for N-peptide of syntaxin-1 in neurotransmitter exocytosis. On the other hand, Munc18-1 harboring point mutations in the hydrophobic pocket region, which abolish the interaction with syntaxin-1 N-peptide, was as effective in rescuing the exocytosis as wild-type Munc18-1, which dismisses the role of the interaction in neurotransmitter release (Meijer *et al.*, 2012). Thus there is a serious dispute in the literature regarding the role of the N-peptide binding in exocytosis, which must be reconciled.

Here we investigate the structural determinants of syntaxin-1A function, with particular emphasis on the interplay between the two binding modes, using PC12 cells and *C. elegans*. Our results reveal a striking interplay between the N-peptide binding mode and the conformational state of syntaxin-1A, and demonstrate that N-peptide plays a critical and complementary role in securing the binary interaction between syntaxin-1 and Munc18-1. Surprisingly, our results also suggest that the N-peptide binding is largely dispensable in exocytosis/membrane fusion.

RESULTS

Double knockdown of syntaxin-1A and 1B leads to significantly reduced neurosecretion accompanied by decreased Munc18-1 level

To examine the combined roles of syntaxin-1A and 1B, we engineered neurosecretory PC12 cells to down-regulate the expression of both isoforms. For this purpose, we used lentivirus-mediated infection of short hairpin RNA (shRNA; Stewart *et al.*, 2003; Han *et al.*, 2009), which was directed against the almost identical mRNA sequence between syntaxin-1A and 1B. After isolation of a heterogeneous population of puromycin-resistant cells, we found that the expression of endogenous syntaxin-1A and 1B in PC12 cells was highly suppressed (Figure 1A). We then examined whether other plasma membrane syntaxins, syntaxin-2 and 4, were up-regulated to compensate for the loss of syntaxin-1A and 1B. We used vasolin-containing peptide (VCP; Peters *et al.*, 1990) and glyceraldehyde-3-phosphate dehydrogenase (GAPDH) as loading controls. We found that the protein levels of the other syntaxins, as well as of the other SNAREs, were not altered in the immunoblot analysis. However, we observed a concurrent decrease in Munc18-1 protein expression (~30%; Figure 1B). This result is consistent with the significant decrease of Munc18-1 in syntaxin-1A–null mice harboring an "open" conformation mutant of syntaxin-1B (Gerber *et al.*, 2008), as well as in syntaxin-1A knockout/1B knockdown neurons (Gerber *et al.*, 2008; Zhou *et al.*, 2013), although the reduction of Munc18-1 in our cells is milder than what was observed in the neurons. We then examined whether neurosecretion from PC12 cells was affected by the depletion of syntaxin-1A/1B. We tested the secretory ability of the syntaxin-1 double-knockdown cells by assaying the release of [^{3}H]noradrenaline (NA) upon stimulation with a high concentration (70 mM) of KCl for 15 min. We observed a 50% reduction in secretion compared with that of control cells, indicating the critical role of syntaxin-1 in exocytosis (Figure 1C).

To better perform rescue experiments with syntaxin-1 mutants, we obtained homogeneous populations of cells by isolating several clonal cell lines from the heterogeneous pool of syntaxin-1 double-knockdown cells exhibiting various degrees of knockdown. The strongest syntaxin-1A/1B depletion phenotype was observed in the single colony, D9, in which a reduction in Munc18-1 expression level was also observed (Figure 1, D and E). To analyze the kinetics of secretion from D9 cells in comparison with the control cells, we evaluated time-course changes of NA release (Figure 1F). In both control (C8) and D9 cells, strong secretion was achieved with a 3-min stimulation, and a plateau followed. The change in the rate of secretion within 3 min of stimulation largely accounts for the impaired NA release in D9 cells. It is also clear that the release of NA persisted despite the high reduction of syntaxin-1 protein expression. Presumably, the remaining secretory activity occurs through the residual syntaxin-1, other plasma membrane syntaxins (i.e., syntaxins-2, 4), or a combination of both. Although our recent results indicate that syntaxin-3 is primarily localized on the vesicular components (Zhu *et al.*, 2013; Bin *et al.*, 2015), previous results from other groups suggest its presence on the plasma membrane (Darios and Davletov, 2006; Sharma *et al.*, 2006), which may also contribute to the residual secretion.

"Open" syntaxin-1A rescues exocytosis more effectively than does wild type, regardless of its significant mislocalization

We next examined whether wild-type syntaxin-1A can be expressed at the appropriate cellular compartment (i.e., the plasma membrane) and rescue secretion defects of D9 cells. We also assessed the effects of conformational switching of syntaxin-1A on its localization and ability to rescue secretion. A previous study showed that the L165A/E166A (LE) mutant form of syntaxin-1A favors to adopt the "open" conformation (Dulubova *et al.*, 1999). This "open"-conformation mutant exhibits an attenuated but not abolished interaction with Munc18-1, the key syntaxin-1–interacting protein (Dulubova *et al.*, 1999, 2003). To express these proteins in D9 cells, we introduced into syntaxin-1A silent nucleotide mutations (SNMs) refractory to the shRNA sequence. D9 cells were infected with lentiviruses that express emerald green fluorescent Protein (EmGFP) alone (control) or wild-type syntaxin-1A or syntaxin-1A LE "open" mutant, and subsequently a heterogeneous pool of blasticidin-resistant cells was isolated. Immunoblot analysis showed similar levels of expression for wild-type (WT) syntaxin-1A and the LE mutant, which were also

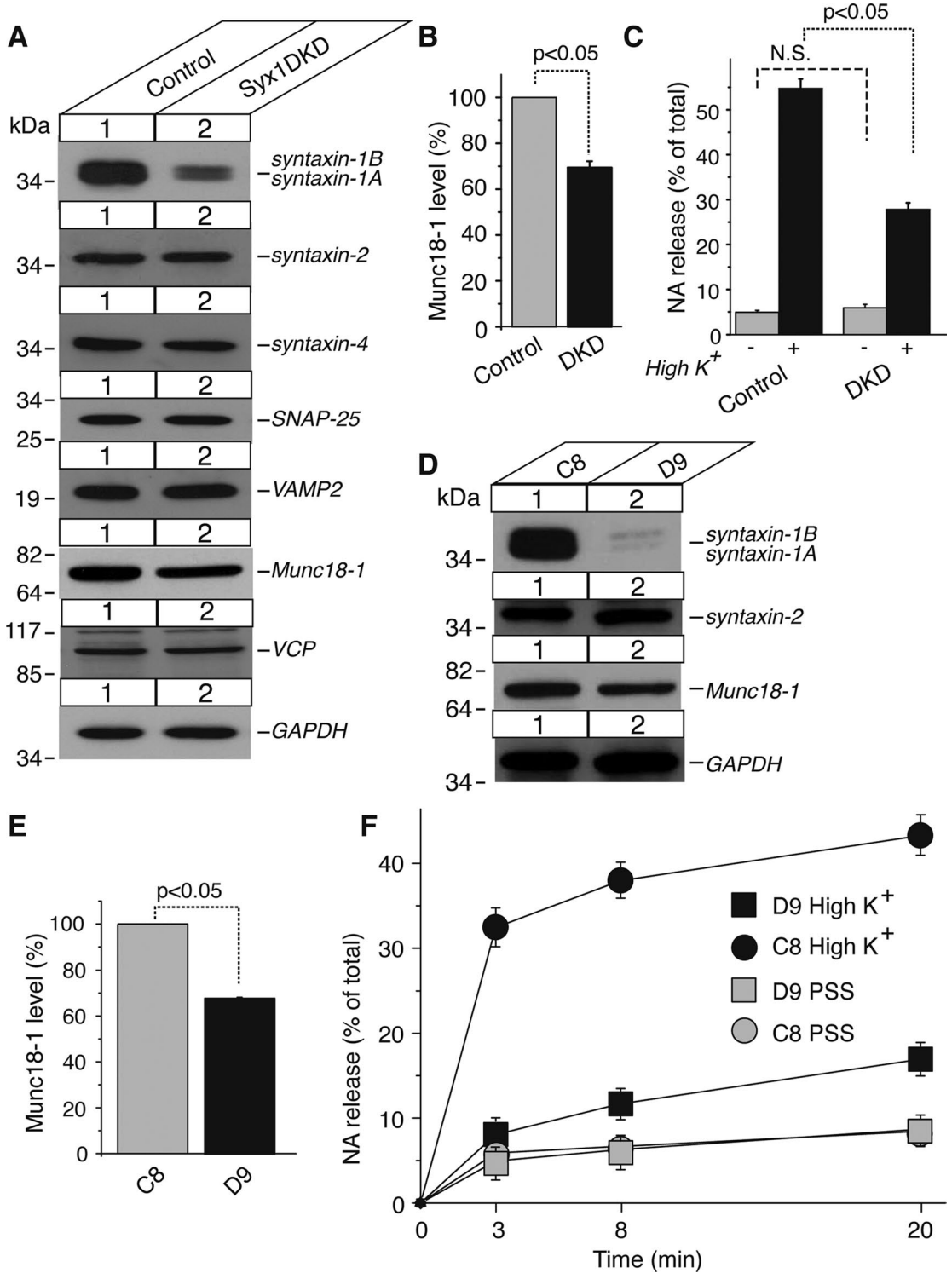

FIGURE 1: Down-regulation of both syntaxin-1A and 1B results in a significant reduction in NA secretion. (A) Immunoblot analysis of a heterogeneous pool of syntaxin-1A/1B double- knockdown cells. We analyzed 20 µg of total homogenates from heterogeneous pools of the control and knockdown cells by SDS–PAGE and immunoblotting using anti-syntaxin-1, 2, and 4, Munc18-1, SNAP-25, synaptobrevin-2, VCP, and GAPDH antibodies. (B) Quantification of the level of Munc18-1 expression in syntaxin-1A/1B–knockdown cells ($t_{(12)} = 5.76$, $p < 0.001$); $n = 4$. (C) NA release from heterogeneous pools of control and syntaxin-1A/1B–knockdown cells upon stimulation with PSS or 70 mM KCl for 20 min ($t_{(12)} = 10.21$, $p < 0.001$); $n = 7$. (D) Immunoblot analysis of the clonal syntaxin-1A/1B double-knockdown (D9) cells. (E) Quantification of Munc18-1 protein level shows a significant decrease in Munc18-1 expression in D9 cells ($t_{(4)} = 3.89$, $p = 0.018$); $n = 3$. (F) Time course of NA release ($t_{(16)} = 10.55$, $p < 0.001$ for 3-min stimulation; $t_{(16)} = 20.68$, $p < 0.001$ for 8-min stimulation; $t_{(16)} = 10.54$, $p < 0.001$ for 20-min stimulation); $n = 9$. [^{3}H]NA-labeled control and knockdown cells were stimulated with PSS or 70 mM KCl for the indicated time (0, 3, 8, 20 min). $p < 0.05$ refers to statistical significance. N.S., not significant. Error bars indicate SEM.

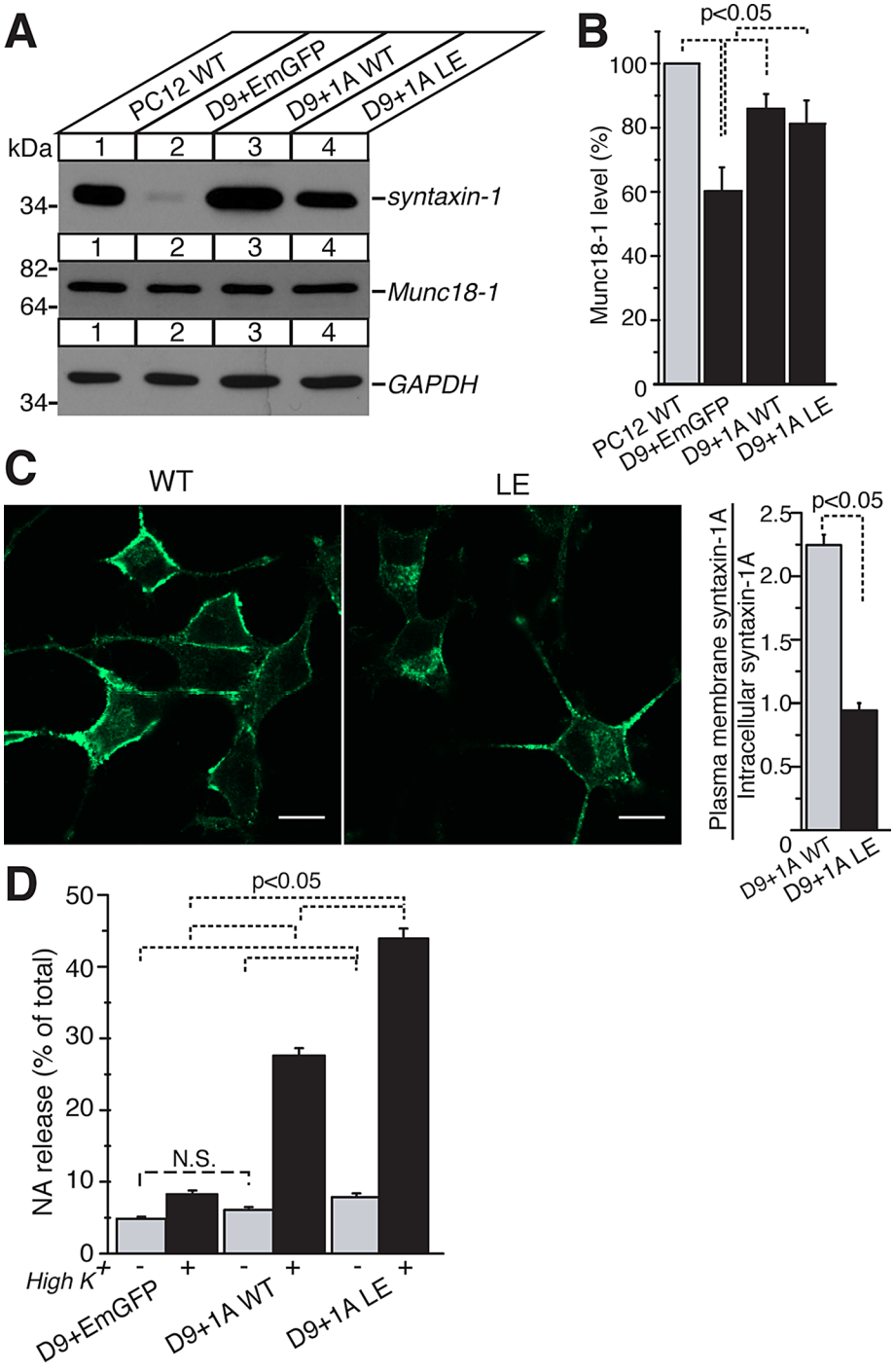

FIGURE 2: Syntaxin-1A LE "open"-conformation mutant effectively rescues the secretory defect of syntaxin-1–depleted cells, although it is intracellularly accumulated. (A) Immunoblot analysis of wild-type syntaxin-1A and syntaxin-1 LE "open" mutant. (B) Quantification of Munc18-1 protein levels upon the reexpression of syntaxin-1A WT and syntaxin-1A LE mutant ($F_{(3,12)} = 4.92$, $p = 0.019$); $n = 4$. (C) Confocal images of wild-type syntaxin-1A and syntaxin-1A LE mutant expressing D9 cells stained with anti–syntaxin-1 antibodies followed by Alexa 488–conjugated goat anti-mouse antibodies. Scale bar, 10 μm. The graph shows the proportion of syntaxin-1 found in the plasma membrane to that found inside the cell that expresses the wild-type or syntaxin-1A LE mutant ($t_{(52)} = 12.97$, $p < 0.001$); $n = 27$ for WT and LE. (D) NA release from D9 cells expressing EmGFP, wild-type syntaxin-1A, or syntaxin-1A LE mutant upon stimulation with 70 mM KCl for 3 min ($F_{(2,39)} = 242.6$, $p = 0$); $n = 6$. $p < 0.05$ refers to statistical significance. N.S., not significant. Error bars indicate SEM.

comparable to the level of endogenous syntaxin-1A in wild-type PC12 cells (Figure 2A). The reduced Munc18-1 protein level was significantly restored upon the expression of syntaxin-1A WT or LE in comparison with EmGFP alone (Figure 2B).

We then visualized the localization of WT syntaxin-1A and syntaxin-1A LE mutant expressed in D9 cells using confocal immunofluorescence microscopy. In D9 cells expressing WT syntaxin-1A, anti–syntaxin-1 antibody detected a strong signal of syntaxin-1A at the plasma membrane, whereas syntaxin-1A LE exhibited significant accumulation in the intracellular compartments (Figure 2C, left). To determine quantitatively the localization (plasma membrane vs. intracellular compartments) of syntaxin-1A WT versus the "open" -conformation mutant, we drew outlines along the plasma membrane of D9 cells expressing these two proteins and measured the intensity of their signals (Supplemental Figure S2 and *Materials and Methods*). We found that the intracellular staining was significantly more pronounced in D9 cells expressing the "open" mutant form than in those expressing the wild type (Figure 2C, left). Note that the mislocalization of the mutant protein is not always observed. As shown in the representative image of the mutant-expressing cells, syntaxin-1 LE mutant is severely mislocalized in the two cells on the left, whereas certain portions of the mutant reach the plasma membrane in the cell on the right. When we examined the distribution of localization index values for D9 cells rescued by expression of the LE "open" mutant (Supplemental Figure S3), we saw two populations (localization index peaks at ~0.65 and ~1.1) in the distribution for the LE open rescued cells, implying that the intracellular trafficking of the LE mutant is variable. The apparently small error bar for the averaged index value of LE (Figure 2C, right) is due to the large number ($n = 27$ for LE and WT) of cells we analyzed.

Regardless of its substantial mislocalization, the open mutant rescued NA secretion significantly better than the wild type in both constitutive (without high K^+) and evoked (with high K^+) release (Figure 2D). This somewhat surprising result is consistent with the findings of a study on knock-in mice expressing the syntaxin-1B "open" conformation mutant (Gerber *et al.*, 2008). These mice exhibited increases in the frequency of miniature excitatory postsynaptic currents (mEPSCs) and in the amplitude of evoked EPSCs (regardless of a decreased size of readily releasable pool). Previously it

was shown that the corresponding mutant form of the *C. elegans* syntaxin-1 homologue UNC-64 displayed the ability to bypass the requirement of UNC-13 in *C. elegans* (Richmond *et al.*, 2001), whereas the mammalian syntaxin-1A mutant was found to bypass the requirement of CAPS1 in priming of dense-core vesicle exocytosis (Liu *et al.*, 2010). These previous and present studies demonstrated that the "open"-conformation mutant form of syntaxin-1 exhibits a gain-of-function trait in both synaptic vesicle and dense-core vesicle exocytosis. One possible explanation for this phenotype is the accelerated formation of the SNARE complex by the "open" mutant (Dulubova *et al.*, 1999; Gerber *et al.*, 2008).

Point mutations of the N-peptide have little effect on the rescue ability of syntaxin-1A

N-peptide of syntaxin is highly conserved among the plasma membrane syntaxin isoforms and species (Figure 3A). To determine the role of syntaxin-1 N-peptide, which interacts with the Munc18-1 hydrophobic pocket, we generated two point-mutant forms of syntaxin-1A. Previous structural studies found that Leu-8 in the N-peptide of syntaxin-1 is the key residue for the interaction between the N-peptide and the hydrophobic pocket of Munc18 (Hu *et al.*, 2007; Burkhardt *et al.*, 2008), as well as for Munc18-1–mediated acceleration of SNARE-dependent membrane fusion (Shen *et al.*, 2007, 2010; Rathore *et al.*, 2010; Figure 3B). In addition, the conserved Asp-Arg-Thr (DRT) motif in the N-peptide has been suggested to stabilize the overall structure of the syntaxin N-peptide/Munc18 complex (Hu *et al.*, 2007; Burkhardt *et al.*, 2008; (Figure 3B). Aspartate-to-arginine mutation at the conserved residue Asp-3 (D3R) abolished the dominant-negative effect of an overexpressed small N-peptide in neurotransmitter release (Khvotchev *et al.*, 2007). Hence, we examined the localization of D3R and L8A mutant forms of syntaxin-1A stably expressed in D9 cells and their ability to rescue the secretion defect in D9 cells. Both D3R and L8A mutants were expressed at a level similar to that of wild-type syntaxin-1A,

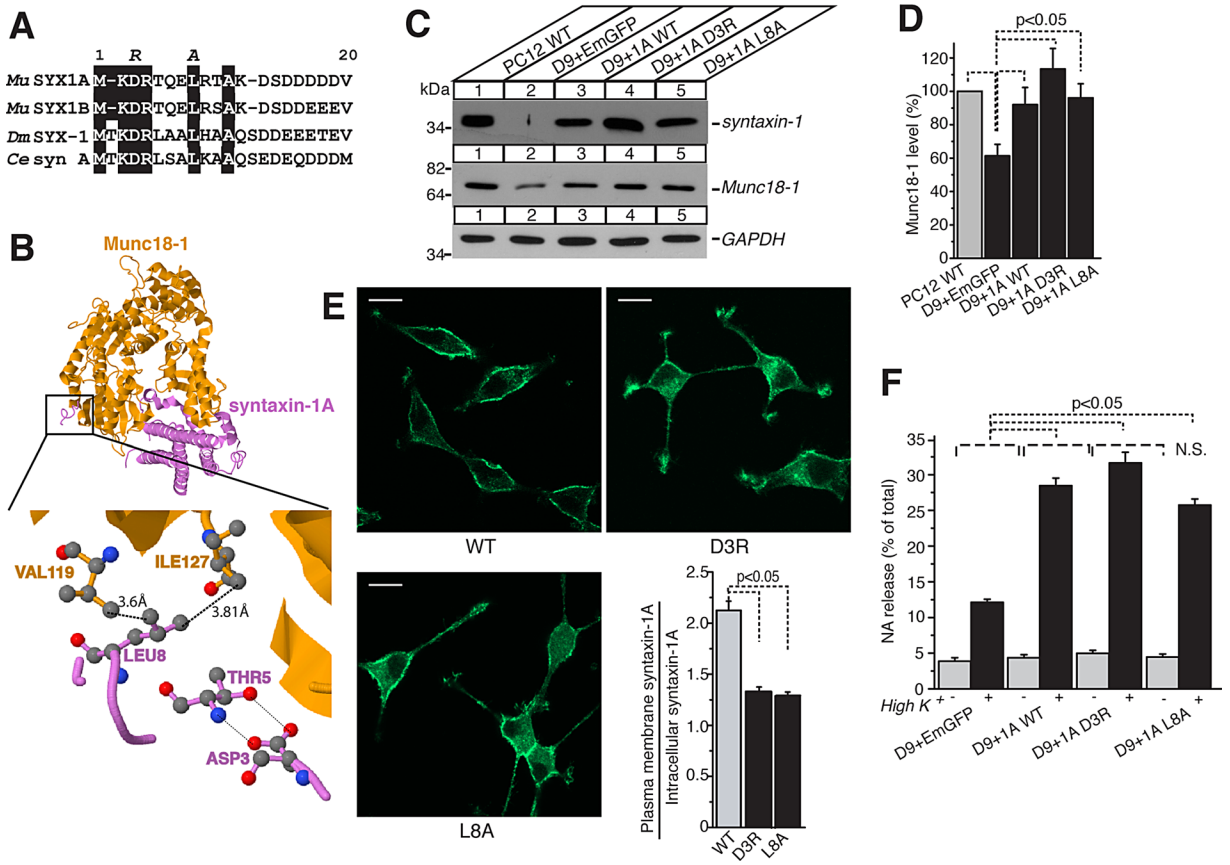

FIGURE 3: N-peptide mutants are significantly accumulated at intracellular compartments but rescue the secretory defect of syntaxin-1–depleted cells. (A) Sequence alignments of the N-terminal 20 amino acids of murine (Mu) syntaxin-1, *Drosophila* (Dm) syntaxin-1, and *C. elegans* (Ce) syntaxin-1. (B) Schematic diagram illustrates the N-terminal peptide of syntaxin-1 binding to the hydrophobic pocket of Munc18-1. Bold dotted lines indicate hydrophobic interactions between syntaxin-1 residues and Munc18-1 residues. Light dotted lines indicate intramolecular hydrogen bonding among syntaxin-1 residues. (C) Immunoblot analysis of D9 cells expressing wild-type syntaxin-1A and D3R and L8A mutants. (D) Quantification of Munc18-1 protein levels upon reexpression of syntaxin-1A WT and D3R and L8A mutants ($F_{(4,15)} = 16.17$, $p < 0.001$); $n = 4$. (E) Confocal images of D9 cells expressing WT and D3R and L8A mutants of syntaxin-1A stained with anti–syntaxin-1 antibodies followed by Alexa 488–conjugated goat anti-mouse antibodies (top and bottom left). Scale bar, 10 μm. Note that the existence of perinuclear localization of syntaxin-1 in addition to its plasma membrane localization is apparent in D9 cells expressing D3R and L8A mutants. The proportion of syntaxin-1 found in the plasma membrane to that found inside the cell that expresses the wild-type and N-terminal mutants of syntaxin-1A (bottom right; $F_{(2127)} = 65.46$, $p = 0$); $n = 36$ for WT, 46 for D3R, and 48 for L8A. (F) NA release from D9 cells expressing WT syntaxin-1 or D3R or L8A mutant ($F_{(3,43)} = 68.38$, $p < 0.001$); $n = 6$. p < 0.05 refers to statistical significance. N.S., not significant. Error bars indicate SEM.

and the expression of these mutants restored the level of Munc18-1 expression (Figure 3, C and D). Unlike the wild type, however, D3R and L8A mutants displayed partial accumulation of staining in perinuclear compartments in addition to the staining at the plasma membrane (Figure 3E, top and bottom left). Quantification of fluorescence signals showed that intracellular staining was significantly more pronounced in D9 cells expressing D3R and L8A mutants than in those expressing the wild type (Figure 3E, bottom right). Nonetheless, both mutants significantly rescued secretion at the level comparable to that of the wild type (Figure 3F). Thus we conclude that the N-peptide binding mode is not absolutely required for dense-core vesicle exocytosis.

Point mutations of N-peptide profoundly inhibit or abolish the rescue ability of syntaxin-1A when this protein adopts the "open" conformational state

We next examined whether the N-peptide point mutants (D3R, L8A) in the "open" conformation state (L165A/E166A, abbreviated as LE) can rescue the secretion defects of D9 cells (Figure 4A). Because our previously mentioned results suggested that N-peptide was dispensable in exocytosis, we originally hypothesized that these mutants would rescue better than wild-type syntaxin-1A, similar to the open-conformation mutant itself (Figure 4C). To our surprise, however, we found that the N-terminal point mutations together with the open-conformation mutations strongly impaired the ability of syntaxin-1A to rescue exocytosis in D9 cells (Figure 4C). We then determined the intracellular localization of these syntaxin-1A mutants in D9 cells. We found them to be severely mislocalized, in that their plasma membrane localization was barely detected (Figure 4D). The results of our N-terminal point mutant studies indicate that the N-peptide plays a crucial role in the localization of syntaxin-1 regardless of the protein's conformational state, but when syntaxin-1 adopts the "open" conformational state, N-peptide is required to rescue secretion. We speculate that N-peptide functions as a safeguard or backup to secure the binary interaction that is mediated primarily between closed syntaxin-1 and Munc18-1 and thereby to secure Munc18-1–dependent regulation of the plasmalemmal localization of syntaxin-1 (Arunachalam *et al.*, 2008; Han *et al.*, 2009). That is, when syntaxin-1 is closed and the closed binding mode is tight enough, N-peptide is largely dispensable. On the other hand, once the "open"-conformation mode is induced in syntaxin-1 and, as a result, the interaction between this protein and Munc18-1 is weakened, the role of N-peptide becomes crucial (see also later discussion of Figure 10). Our immunoblot data (Figures 2A, 3C, and 4A) indicated that the level of the syntaxin-1A variants expressed in the KD cells is similar to the endogenous level of syntaxin-1 in PC12 cells. Thus the functional difference among the syntaxin-1A variants does not seem to be explained by the difference in their expression level.

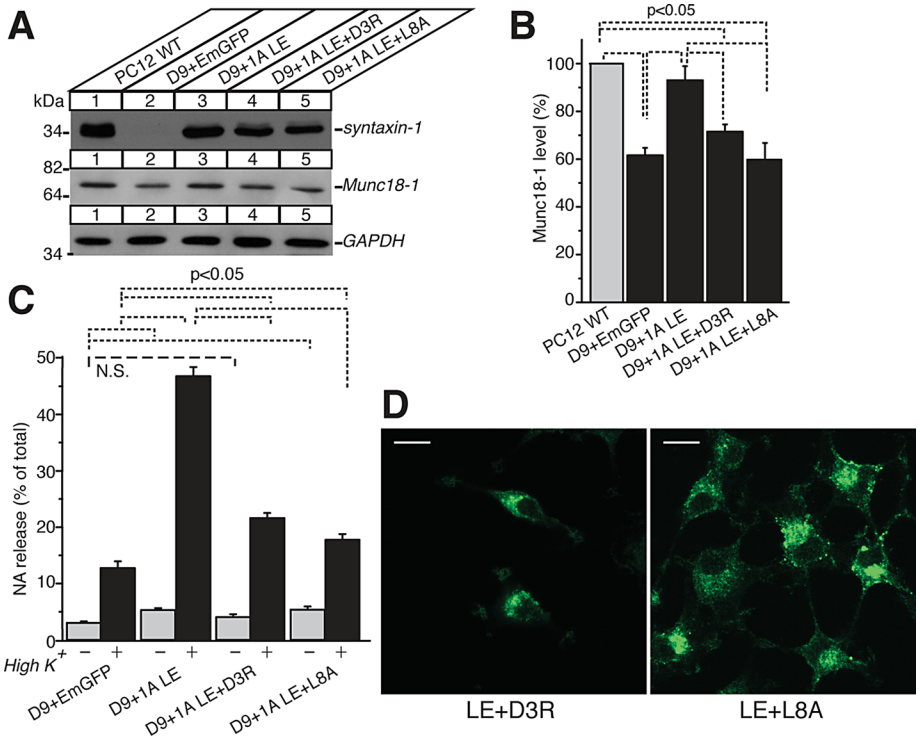

FIGURE 4: N-peptide mutations abolish the secretion rescue ability of syntaxin-1A adopting the "open" conformation and further impair its localization. (A) Immunoblot analysis of D9 cells expressing syntaxin-1A LE "open" mutant without and with additional N-terminal point mutations (D3R and L8A). (B) Quantification of Munc18-1 protein levels upon expression of syntaxin-1A LE "open" mutant without and with the additional N-terminal point mutations ($F_{(4,10)} = 16.58$, $p < 0.001$); $n = 3$. (C) NA release from D9 cells expressing syntaxin-1A LE "open" mutant with and without the additional N-terminal point mutations ($F_{(3,20)} = 156.9$, $p < 0.001$); $n = 6$. (D) Confocal images of D9 cells expressing syntaxin-1A LE "open" mutant with D3R (left) and L8A (right) stained with anti–syntaxin-1 antibodies followed by Alexa 488–conjugated goat anti-mouse antibodies. Scale bar, 10 μm. Note that strong signals are detected from intracellular compartments, whereas signals from the plasma membrane and extended neurites were barely detectable in the two mutant-expressing cells. $p < 0.05$ refers to statistical significance. N.S., not significant. Error bars indicate SEM.

Mammalian syntaxin-1A can rescue the lethal phenotype observed at the first larval stage of *C. elegans unc-64*–null mutants

The results obtained from our PC12 cell studies suggest that the N-peptide of syntaxin-1 is critical for the protein's trafficking to the plasma membrane when syntaxin-1 adopts an open conformational state. Surprisingly, our results also suggest that the N-peptide binding mode is dispensable for exocytosis. There is a concern, however, that the presence of other plasmalemmal syntaxins isoforms, such as syntaxin-2, in mammalian neurons and neuroendocrine cells may have compensatory actions, which make the role of syntaxin-1 N-peptide apparently less important. Another key question is how our results are translated into the in vivo system, including a behavioral outcome.

To address these issues, we performed a structural and functional analysis of mammalian syntaxin-1 using *C. elegans*. Previously the syntaxin-1–interacting protein Munc18-1 was shown to rescue the uncoordinated, paralytic phenotype of *C. elegans unc-18*–null mutants (Gengyo-Ando *et al.*, 1996). Thus we asked whether expression of mammalian syntaxin-1A WT in the entire nervous system can rescue the lethal phenotype of the *unc-64*–null mutant worms. UNC-64 in *C. elegans* is an orthologue of mammalian syntaxin-1 and is the sole isoform expressed in neurons. *unc-64*–null mutants are unable to move and develop beyond the first larval stage (Saifee *et al.*, 1998). To determine

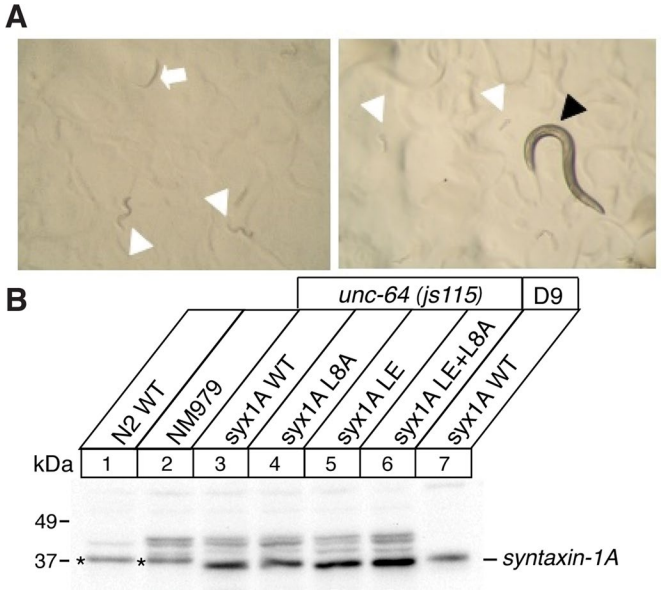

FIGURE 5: Expression of mammalian syntaxin-1A variants rescues paralysis and arrested development of *C. elegans unc-64*–null mutants. (A) Expression of mammalian wild-type syntaxin-1A is sufficient to rescue the lethal phenotype of *unc-64*–null mutants. The white arrow indicates an *unc-64*–null mutant in the first larval (L1) stage. White arrowheads indicate L1 *unc-64*–null mutants rescued by expression of mammalian syntaxin-1A WT. The black arrowhead indicates an adult worm expressing mammalian syntaxin-1A WT in the *unc-64*–null mutant background. (B) Immunoblot analysis of *unc-64 (js115)*–null mutants expressing various forms of mammalian syntaxin-1A. I378 polyclonal antibody against syntaxin-1A was used to detect the various syntaxin-1A forms. Asterisks indicate endogenous UNC-64, which has a slightly larger molecular weight than mammalian syntaxin-1A, expressed in N2 and NM979 control strains. The band in the last lane of the immunoblot indicates syntaxin-1A WT reexpressed in syntaxin-1A/1B double-knockdown (D9) PC12 cells.

whether mammalian syntaxin-1A is sufficient to rescue the lethal null-mutant phenotype, we designed an expression construct to drive expression of syntaxin-1A under the control of a panneuronal promoter, *Prgef-1*. This construct was injected into the gonads of young adult worms of the NM979 strain (genotype *unc-64(js115)/bli-5(e518) III*), together with a coinjection marker encoding red fluorescent protein (RFP), whose expression was driven by a muscle-specific promoter (*Materials and Methods*). We found that the neuronal expression of the mammalian syntaxin-1A WT transgene rescues the lethal phenotype of *unc-64*–null mutants. The *unc-64*–null mutant worms expressing the mammalian syntaxin-1A WT were able to move, grow, and reproduce (Figure 5A; also see Figures 6 and 7). This striking rescuing ability of mammalian syntaxin-1A allowed us to examine directly the structural determinants of syntaxin-1 function in vivo without the confounding presence of other neuronal syntaxin isoforms.

Point mutations of N-peptide specifically abolished the rescuing activity of the "open" syntaxin-1A of *unc-64*–null mutants

We next examined the effects of the N-peptide mutations on syntaxin-1A function using the in vivo *C. elegans* system. The mammalian syntaxin-1A mutants tested in *C. elegans* included syntaxin-1A carrying single D3R or L8A point mutations in the N-peptide, syntaxin-1A favoring an "open" conformation upon the L165A/E166A (LE) double mutation, and syntaxin-1A favoring the "open" conformation while carrying the L8A mutation (LE+L8A; Table 1). We were able to establish transgenic lines expressing each mutant syntaxin in *unc-64*–null mutants. However, we also encountered difficulties in isolating those rescued by expression of syntaxin-1A LE+L8A. After an intensive search for LE+L8A lines, we managed to isolate three lines, of which only one could be maintained during the course of the study. In addition, the syntaxin-1A LE+L8A–rescued lines exhibited several distinct phenotypes, such as slow locomotion, a severe egg-laying defect, and slow growth/propagation rate, compared with the lines rescued by the other syntaxin-1A variants (see later discussion).

Construct	Transgenic lines	Phenotypic rescue
Panneuronal mammalian syntaxin-1A WT	Yes	Development and locomotion rescued
Panneuronal mammalian syntaxin-1A D3R	Yes	Development and locomotion rescued
Panneuronal mammalian syntaxin-1A L8A	Yes	Development and locomotion rescued
Panneuronal mammalian syntaxin-1A LE	Yes	Development and locomotion rescued and mild egg-laying defect
Panneuronal mammalian syntaxin-1A LE+L8A	Yes	Development rescued but severe egg-laying and locomotion defects

TABLE 1: Phenotypic rescue of *unc-64*–null mutants by expression of mammalian syntaxin-1 variants.

To provide evidence for the expression of mammalian syntaxin-1A variants, we performed Western blot analysis of the whole-protein extracts prepared from the rescued lines using the polyclonal anti–syntaxin-1 antibody (I378; Dulubova *et al.*, 1999; Figure 5B). The bottom band in each of the lanes was detected at the same size as WT syntaxin-1A expressed in D9 cells, indicating that the bottom band corresponds to mammalian syntaxin-1A. Note that the band with a slightly higher molecular weight than that of mammalian syntaxin-1A was detected in the lanes of N2 WT strain and the heterozygous, balanced NM979 strain (Figure 5B). Considering that mammalian syntaxin-1A and UNC-64 share a high amino acid identity (Ogawa *et al.*, 1998; Saifee *et al.*, 1998) and that UNC-64 (*C. elegans* Sequencing Consortium, 1998) contains three more amino acids than syntaxin-1A, the higher band recognized by the polyclonal antibody is likely to correspond to endogenous UNC-64. The absence of this band in the rescued lines confirmed that all of the rescued lines were established on the *unc-64*–null background. We noted that the intensity of the band corresponding to syntaxin-1A LE+L8A mutant was higher than that of the other syntaxin-1A variants. We also found unusually high RFP signals (the coinjection marker) in *unc-64*–null mutants rescued by the LE+L8A mutant, indicating a high expression level for the transgene. We speculate that the high level of this mutant protein expression is necessary to rescue the lethal, paralytic phenotype of *unc-64*, presumably due to the poorer rescue ability of this mutant compared with the other syntaxin variants.

To quantify the level of rescue of the paralytic phenotype in *unc-64*–null mutants by syntaxin-1A variants, we performed locomotion assays on the rescued lines, as well as on the N2 WT worms (Figure 6). Several rescue lines expressing a syntaxin-1A variant

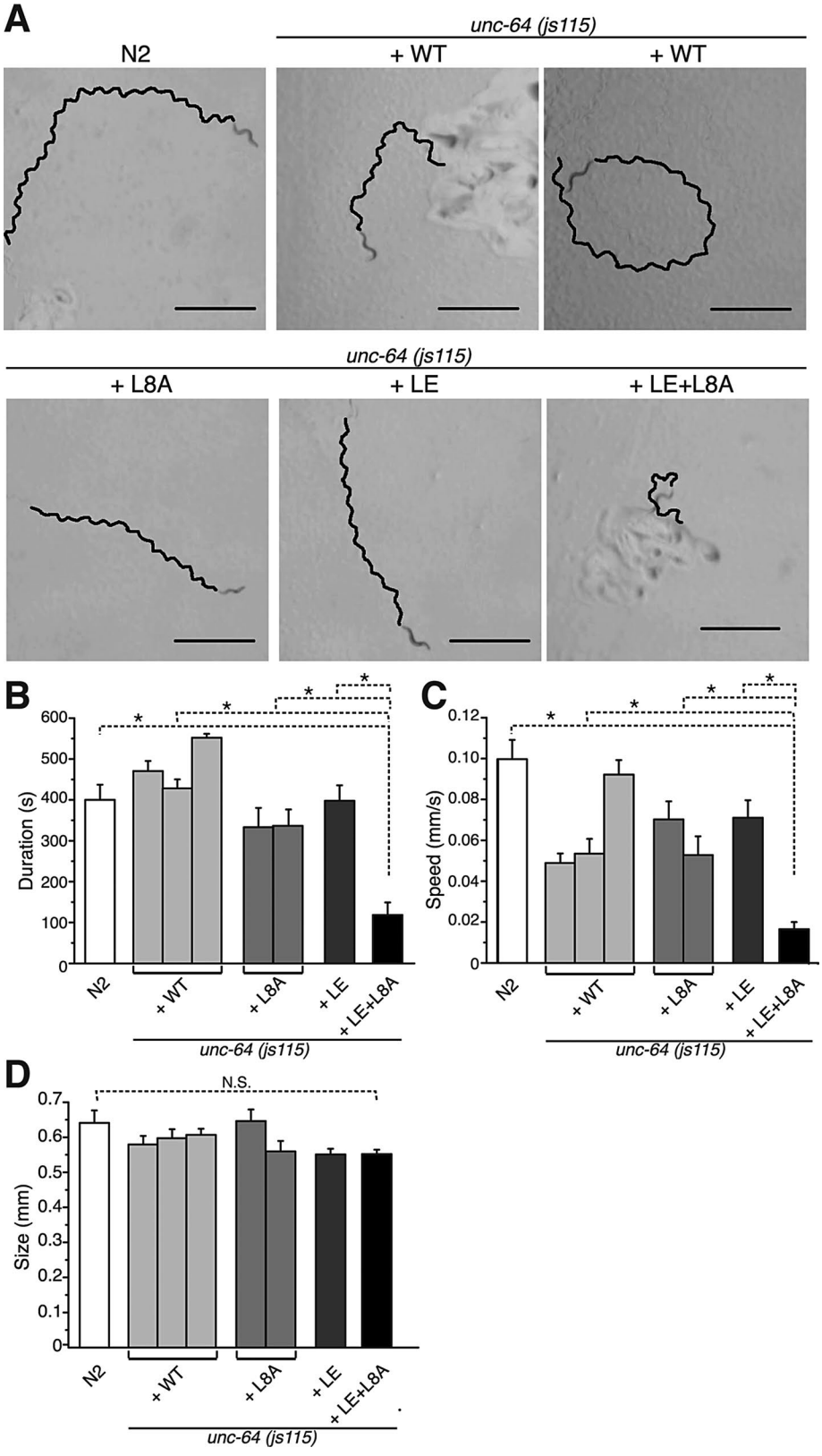

FIGURE 6: An N-peptide point mutation disrupts the ability of "open" syntaxin-1A to rescue the locomotion of *unc-64*–null mutants in late larval stage. (A) Representative 60-s traces of N2 and *unc-64*–null mutants expressing mammalian syntaxin-1A variants taken from 10-min video recordings. The null mutants expressing wild-type syntaxin-1A from two different transgenic lines (top middle and right) were examined for their locomotion. Scale bars, 1 mm. (B) Average duration of active locomotion during 10-min video recordings of N2 and *unc-64*–null mutant animals expressing mammalian syntaxin-1A variants ($F_{(7,87)} = 16.71$, $p < 0.001$); $n = 10$ for N2, 11–13 for WT, 9–13 for L8A, 13 for LE, and 14 for LE+L8A. The number of bins represents the number of different transgenic lines used in this analysis. (C) Average speed of the animals within the 60-s representative time period ($F_{(7,85)} = 13.93$, $p < 0.001$); $n = 10$ for N2, 11–13 for WT, 9–11 for L8A, 13 for LE, and 14 for LE+L8A). (D) The size (body length) of each animal examined for its locomotion in the foregoing analyses was within a similar range ($n = 10$ for N2, 11–13 for WT, 9–11 for L8A, 13 for LE, and 14 for LE+L8A). *$p < 0.05$ compared with control. N.S., not significant. Error bars indicate SEM.

exhibited variations, presumably due to differential expression levels. To accommodate these variations among rescue lines, we examined worms from a few rescue lines for each variant. We selected seven rescue lines (three lines for WT, two for L8A, one for LE, and one for LE+L8A). We recorded the locomotion of the L4 larvae ($n > 10$ for each line) for 10 min after transferring them to nematode growth medium (NGM) plates seeded with fresh OP50 bacteria lawns. We then analyzed the duration of active locomotion (Figure 6B) and the average speed during active 1-min locomotion (Figure 6C). We found that L4 larvae of N2 exhibit active locomotion on average for ~400 of the 600-s recording time. Two of the syntaxin-1A WT–rescued lines, the L8A lines, and the LE line exhibited similar durations of active locomotion. However, one of the syntaxin-1A WT rescued lines (bin 3 for WT in Figure 6B) showed a significantly longer duration of active locomotion for ~540 of the 600-s recording. In contrast, LE+L8A exhibited an active locomotion only for ~200 s. With regard to the average speed of locomotion, N2 showed the fastest speed of ~1.0 mm/s, and the strongest syntaxin-1A–rescued line (bin 3 for WT in Figure 6B) reached a similar speed (Figure 6C). However, all of the other rescue lines expressing WT, the L8A mutant, or the LE mutant exhibited 50–75% of the average speed of N2, indicating their incomplete rescue ability. Again, the LE+L8A mutant exhibited a distinctly slow speed of <20% of the speed of N2.

The locomotion traces indicated that the rescued worms, except for the LE+L8A mutant, displayed relatively smooth sinusoidal movement, which is comparable to the movement of WT (Figure 6A). The LE+L8A mutant often exhibited loopy traces, which were occasionally observed in the other rescued lines. The size of the L4 larvae used for the locomotion assay was similar among the rescued lines and N2 (Figure 6D). Thus our results demonstrate that the strongly

rescued line by syntaxin-1A WT (bin 3) can exhibit similar or even higher locomotion activity compared with N2. Furthermore, our results suggest that N-peptide mutation or open-conformation mutation alone causes relatively mild effects on the ability of syntaxin-1A to rescue the paralytic phenotype of *unc-64*–null *C. elegans*. In contrast, mutation of both (LE+L8A) causes distinctly poor ability to rescue locomotion.

In addition to the slow locomotion, we also observed that most of the worms expressing the LE+L8A mutant exhibited a severe egg-laying defect (Table 1). This egg-laying defect caused those worms to appear sick due to the build-up of eggs inside the body. Eventually, unlaid eggs hatched inside the worms, killing the parental worms. This defect was also occasionally observed in "open" syntaxin-1A (LE)–expressing worms, whereas it was barely found in the worms rescued by WT or N-peptide mutants (Table 1). To measure quantitatively the growth/propagation phenotype, we counted the rescued L4 and adult worms expressing mammalian syntaxin-1A variants (WT, L8A, LE, and LE+L8A) over a period of 9 d (Figure 7; *Materials and Methods*). We selected eight rescue lines (two for WT, two for L8A, two for LE, and two for LE+L8A) for the two sets of counting (Figure 7). *Unc-64*–null mutant worms expressing syntaxin-1A L8A mutant did not increase in population size as effectively as the WT-expressing worms, indicating that L8A mutation slightly impaired syntaxin-1A function in vivo. Similarly, *unc-64*–null mutant worms expressing LE "open" syntaxin-1A did not produce as many progeny as the WT-expressing worms. As expected from the observation of phenotypic rescue, worms expressing LE+L8A mutant produced a strikingly low number of progeny, presumably due to the severe egg-laying defect (Figure 7 and Table 1). We also found that LE+L8A mutants exhibited slower developmental growth, which also contributed to the slower propagation. Thus our in vivo data on locomotion and brood-size assays are consistent with our observations from the PC12 cells in that N-terminal mutation alone has a limited effect on the locomotion and growth of *C. elegans*, whereas the same mutation in the open-conformation background severely impairs locomotion, propagation, and growth regardless of its enhanced expression level (Figures 6 and 7 and Table 1).

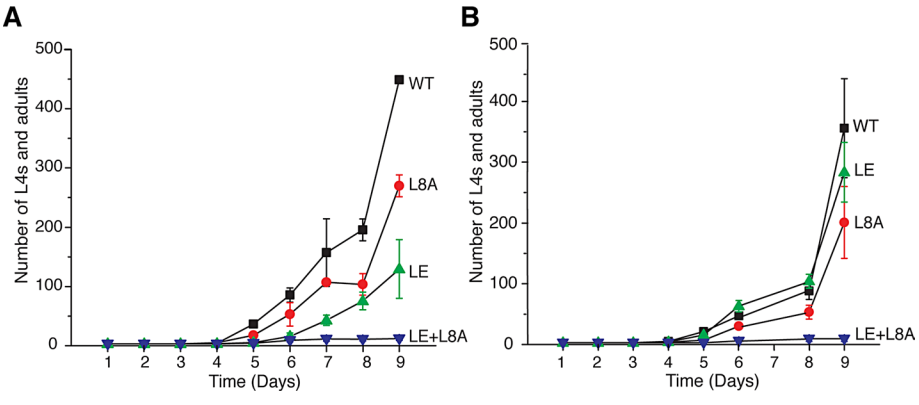

FIGURE 7: The differential propagation of *unc-64*–null mutants expressing various forms of mammalian syntaxin-1A. (A and B) Growth curves of *unc-64*–null mutant worms expressing syntaxin-1A WT, L8A, LE, or LE with the additional L8A mutation. Over a period of 9 d, the L4 and adults grown in plates of these worms were counted every day ($n = 3$). Since variations exist among transgenic lines, the brood size was assessed in two rounds. In other words, different transgenic lines expressing each variant were used in A and B. *unc-64*–null mutant worms expressing either the WT or LE+L8A consistently produced the greatest and least number of progeny, respectively. The null-mutant worms expressing the L8A or LE mutant produced an intermediate number of progeny. Error bars indicate SEM.

In our PC12 cell studies, we suggested that the inability to rescue secretion of LE+L8A mutant is largely due to the severe intracellular mislocalization of this mutant protein. Is the poor rescue ability of the same mutant in *C. elegans* also due to its mislocalization in the neurons? We performed immunohistochemistry using the polyclonal antibody (I378). This antibody detected consistent expression of syntaxin-1A variants in the nervous system, including the nerve ring in the head region, the ventral nerve cord spanning from the head to the tail, and the tail region. However, the staining of this antibody also suffered from the high background (unpublished data), which prevented us from analyzing the intracellular localization of the syntaxin-1A variants in *C. elegans* neurons.

L8A mutation in N-peptide of "open" syntaxin-1A dramatically impairs the interaction with Munc18-1

We finally asked why the function of N-peptide is dramatically different depending on the conformational state of syntaxin-1 in PC12 cells and *C. elegans*. Before investigating potential mechanisms that might explain the interplay between N-peptide and the conformational state of syntaxin-1, we hypothesized that mutations introduced in both the N-peptide and the conformational state would severely impair the binary interaction between monomeric syntaxin-1A and Munc18-1, whereas mutations in either N-peptide or the conformational state would only have limited effect on the interaction (see later discussion of Figure 10). This hypothesis was based on our previous finding that the degree of binary interaction between Munc18-1 and monomeric syntaxin-1 is positively correlated with the degree of the plasmalemmal localization of syntaxin-1 (Han *et al.*, 2011).

To examine the binary interaction between syntaxin-1A variants and wild-type Munc18-1, we first performed glutathione *S*-transferase (GST) pull-down experiments using a cytoplasmic region of syntaxin-1A (residues 1–264). In these experiments, we examined whether GST–syntaxin-1A could quantitatively pull down Munc18-1, which was exogenously expressed in HEK-293 cells (Figure 8A). We found that L8A or L165A/E166A (LE) "open" mutations in syntaxin-1A caused partial reductions in its binding ability to Munc18-1, whereas a combination of L8A and LE mutations strongly abolished binding. To achieve more quantitative GST pull downs, we also examined whether GST–syntaxin-1A (1–264) shows a similar binding profile toward bacterially expressed Munc18-1–hexahistidine (His_6). Here we titrated different concentrations of Munc18-1–His_6 for the binding to GST–syntaxin-1A (Figure 8B). We found that the binding affinity of syntaxin-1A variants with Munc18-1–His_6 was in this order: WT > L8A > LE >> LE+L8A. This pattern is similar to the one observed in the experiments using the Munc18-1 expressed in HEK-293 cells, in that double mutation of LE+L8A strikingly abolished the ability of syntaxin-1A to bind to Munc18-1–His_6.

To determine the thermodynamics of the binding between syntaxin-1 variants and Munc18-1, we also performed isothermal titration calorimetry (ITC) experiments using recombinant syntaxin-1A (1-265)–His_6 and Munc18-1–His_6 (Figure 9 and Table 2). We found that as wild-type syntaxin-1A (1-265)–His_6 molecules were injected into the sample

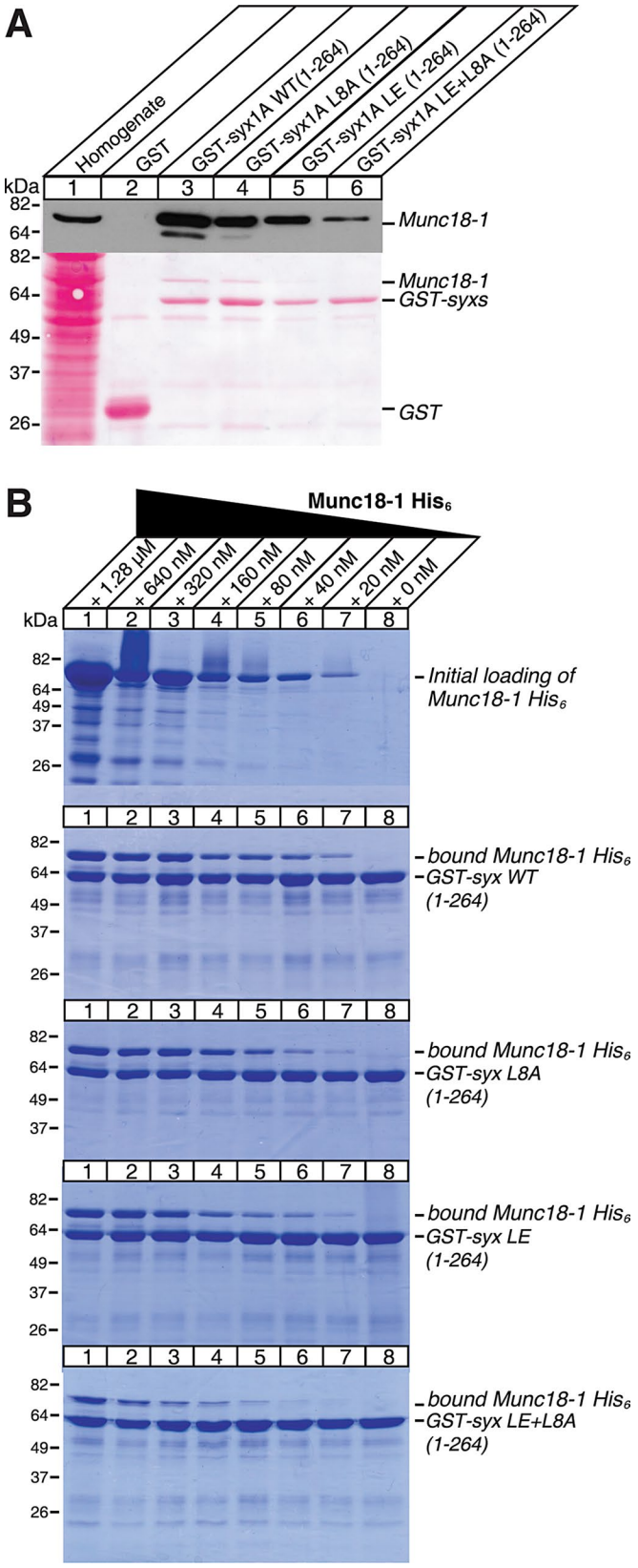

FIGURE 8: N-peptide of syntaxin-1 differentially engages in its interaction with Munc18-1, depending on its conformation. (A) GST pull-down assay of Munc18-1 by a variety of GST fusion forms of syntaxin-1A (1-264). HEK293 cells expressing exogenous Munc18-1 through transient transfection were harvested and homogenized. The resulting supernatant containing soluble Munc18-1 protein was incubated overnight with purified syntaxin-1A GST-fusion proteins immobilized on glutathione agarose. Munc18-1–bound GST–syntaxin-1A was subjected to SDS–PAGE and immunoblotting (top). Homogenate lane shows exogenously expressed Munc18-1 before the pull-down assay. Inputs of homogenate, GST alone (control), and GST-syntaxin-1A proteins were visualized by Ponceau S staining (bottom). (B) Coomassie blue staining of His_6-tagged Munc18-1 pulled down by WT and mutant forms of GST-syntaxin-1A (1-264). Before staining, these GST-fusion proteins were incubated with various concentrations (range, 0 nM to 1.28 µM) of His_6-tagged Munc18-1, which was purified from bacteria.

cell of the ITC apparatus that did not contain the recombinant Munc18-1 protein, a substantial amount of exothermal signal was measured (Figure 9A). This is likely to reflect the dissociation of multimerized syntaxins that were subject to significant dilution upon injection (Lerman *et al.*, 2000; Deák *et al.*, 2009). The multimerization signal was also observed for the L8A and LE mutants but not for the LE+L8A mutant. Thus, in our thermodynamic parameter calculations and integration data, we subtracted the value associated with the multimerization from that of the binding with Munc18-1 (Figure 9, B–E). Our ITC data indicated that L8A mutant syntaxin-1A was moderately defective in Munc18-1 binding, with slightly reduced binding enthalpy (ΔH; –23.5 ± 1.3 kcal compared with –29.5 ± 1.6 kcal for WT) and mildly decreased binding affinity (K_d; 19.1 ± 1.7 vs. 12.8 ± 8.1 nM for WT; Table 2). Despite the marginally reduced energies and binding affinity, the L8A mutant still exhibited $N = 1.0 \pm 0.1$, indicating that there was still 1:1 stoichiometric interaction toward Munc18-1 (Table 2).

The LE "open" mutant showed much more severe defects in Munc18-1 interaction, with considerably lower binding enthalpy of –13.7 ± 1.4 kcal and largely elevated dissociation constant of 196.3 nM. Binding affinity of the LE mutant for Munc18-1 is ~15 times lower than that of WT in our assays. This reduction is somewhat larger than what Burkhardt *et al.* (2008) found. In their ITC analysis, K_d for the WT was 1.4 nM, whereas K_d for the LE was 7.7 nM, indicating that this ~5.5-fold reduction in binding affinity is caused by the LE mutation. When the affinity was measured by analytical ultracentrifugation, a more dramatic decrease was observed for the LE mutant: K_d = 20 nM for WT syntaxin-1 and 2.2 µM for the LE mutant (Josep Rizo, University of Texas Southwestern Medical Center, Dallas, TX, personal communication). Although the degree of decrease in binding affinity appears to vary depending on the experimental conditions, there is a consistent, substantial decrease in the affinity by the LE mutation. In addition, we found the LE "open" mutant exhibited substantially different stoichiometry in the binding from that of WT or L8A mutant, with $N = 0.4 \pm 0.02$. When we simulated the interaction at $N = 1$, the model did not fit well (Supplemental Figure S4 and Table 2), suggesting that the stoichiometry may not be 1:1 for this specific mutant. As stated earlier, the entire syntaxin-1A cytoplasmic domain is known to multimerize in the in vitro environment. The K_d for oligomerized syntaxin-1A (1-265) measured by analytical ultracentrifugation was reported to be in the low-micromolar range (Lerman *et al.*, 2000), which is comparable to the K_d for the binding between the LE mutant and Munc18-1 (Josep Rizo, personal communication). We speculate that equilibrium was established between syntaxin-1A–syntaxin-1A interaction and syntaxin-1A–Munc18-1 interaction in our ITC experiment. That is, as the LE mutant was repeatedly injected into the cell of ITC, its local concentration within the cell increased, which favored syntaxin-1A oligomerization. The oligomerized syntaxin-1A was presumably unable to bind

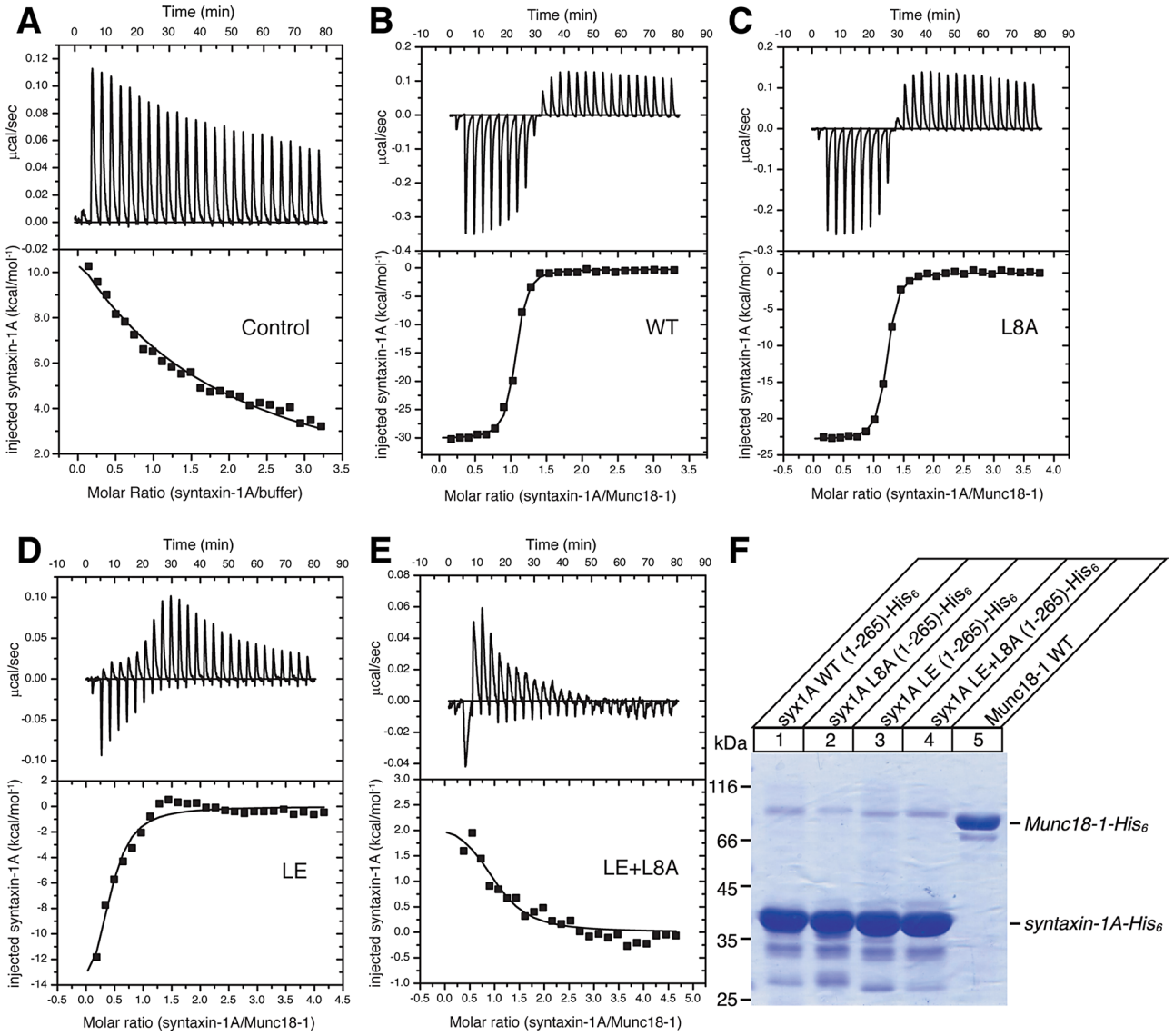

FIGURE 9: A point mutation in N-peptide of syntaxin-1 differentially alters the binding affinity for Munc18-1, depending on its conformation. (A) Isothermal calorimetry analysis of binding between His_6-tagged syntaxin-1A (1-265) molecules. (B–E) ITC analysis of the binding between various forms of His_6-tagged syntaxin-1A (1-265) and His_6-tagged Munc18-1. Representative raw ITC data (top) and integrated and normalized ITC data (bottom). (F) Coomassie-stained SDS–PAGE gel run with the proteins used in ITC experiments.

Munc18-1 effectively, and thus did not occupy the entire binding site of Munc18-1. It is likely that the anomalous stoichiometry of the interaction between the LE mutant and Munc18-1 was simply due to a competing process (i.e., syntaxin oligomerization) of the mutant. In other words, the true stoichiometry of the two proteins could have been 1:1, but the observed stoichiometry of $N = 0.4$ was found because their interaction was partially hampered by the oligomerization of the LE mutant.

Strikingly, we found that LE+L8A mutant displayed very poor binding to Munc18-1 (K_d = 2.9 ± 2.9 µM). Taken together, these

Syntaxin-1A variant	Δ*H* (kcal/mol)	−*T*Δ*S* (kcal/mol)	Δ*G* (kcal/mol)	K_d (nM)	*N*
WT	−29.5 ± 1.59	18.6 ± 2.02	−10.9 ± 0.55	12.8 ± 8.14	1.0 ± 0.01
L8A	−23.5 ± 1.30	13.1 ± 1.26	−10.4 ± 0.13	19.1 ± 1.74	1.0 ± 0.06
LE	−13.7 ± 1.36	3.5 ± 1.41	−9.2 ± 0.18	196.3 ± 52.14	0.4 ± 0.02
LE+L8A	26.2 ± 17.38	−31.2 ± 16.04	−5.0 ± 3.26	28,683.0 ± 28,570.96	1.0 ± 0.09
When fitted to *N* = 1					
LE	−6.6 ± 0.39	−2.5 ± 0.76	−9.1 ± 0.39	141.0 ± 122.67	1.0

TABLE 2: Binding parameters of syntaxin-1A variants with Munc18-1.

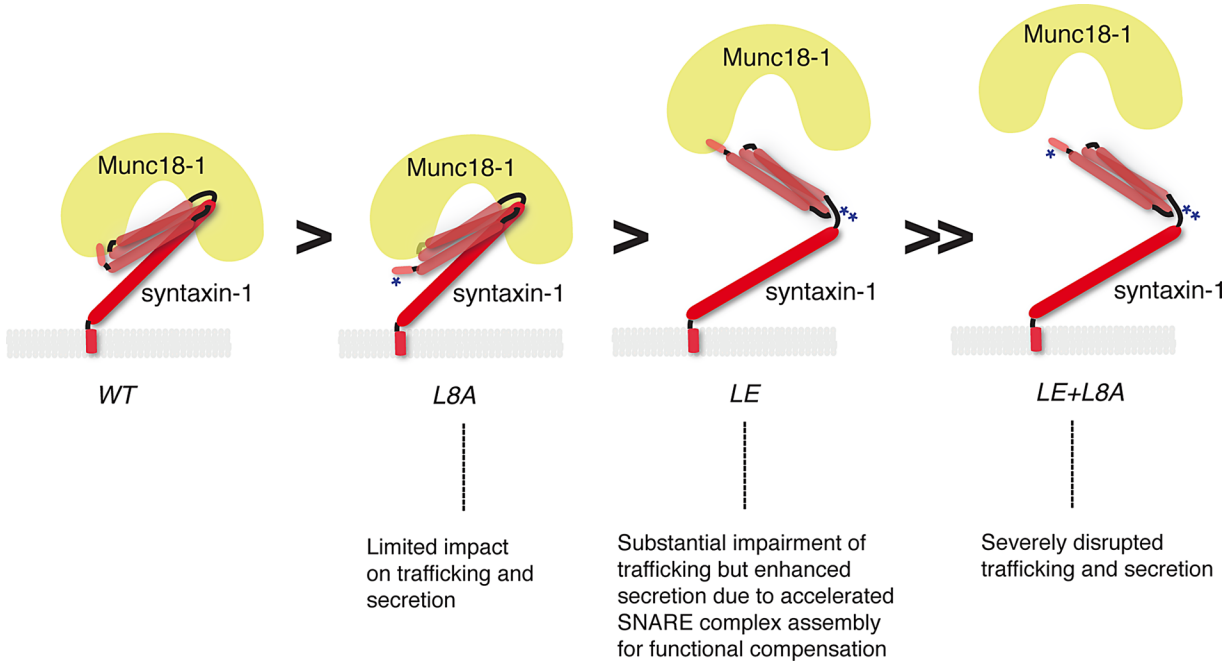

FIGURE 10: Schematic diagram illustrates the strength of interaction between syntaxin-1A variants and Munc18-1. The strength of protein–protein interaction decreases from left to right. The strongest interaction is achieved with wild-type syntaxin-1 (far left), whereas the LE "open" mutant form of syntaxin-1 with the additional L8A mutation results in significant displacement of Munc18-1 (far right). Asterisks indicate mutations.

results indicate that L8A mutation by itself does not strongly disrupt the interaction of syntaxin-1A with Munc18-1. However, when the identical mutation is introduced in LE "open" conformation of syntaxin-1A, it almost abolishes the binding to Munc18-1, indicating that the crucial function of N-peptide in the "open" state of syntaxin-1A is to mediate interaction with Munc18-1. Collectively our ITC data are in full agreement with aforementioned GST pull-down experiments, thus adding confidence that there are reductions in binding affinity and binding enthalpy in the order of WT > L8A >> LE >>> LE+L8A. Thus, our biochemical results support our hypothesis that N-peptide plays a critical complementary role in securing the binary interaction between syntaxin-1 and Munc18-1 and thereby the regulation of intracellular localization of syntaxin-1 by Munc18-1 (Figure 10).

DISCUSSION

In this study, we discovered the surprising interplay between the conformational state of syntaxin-1A and the role of its N-peptide binding toward Munc18-1. In the WT ("closed") conformation, point mutations of N-peptide have little effect on the ability of syntaxin-1A to rescue exocytosis in PC12 cells (Figure 3F), as well as to rescue lethality, movement, and growth in *C. elegans* (Figures 6 and 7). In contrast, introduction of N-terminal mutations in syntaxin-1A favoring the "open" conformation profoundly inhibits or abolishes this protein's rescuing ability and plasmalemmal localization in PC12 cells (Figure 4, C and D), as well as its ability to rescue locomotion and growth in *C. elegans* (Figures 6 and 7). We sought to rationalize our results with the present hypotheses on the function of syntaxin-1 N-peptide, which is known to bind to the outer surface of hydrophobic pocket of Munc18 (Hu *et al.*, 2007; Burkhardt *et al.*, 2008). At least two different hypotheses had been proposed regarding the role of syntaxin-1 N-peptide: 1) it is essential for Munc18-1–mediated priming of SNARE-dependent fusion by allowing the binding of Munc18-1 to the SNARE complex (Burgoyne and Morgan, 2007; Südhof and Rothman, 2009) (Supplemental Figure S1A), and 2) it secures the Munc18-1/"closed" syntaxin-1 complex to block the formation of ectopic SNARE complexes (Burkhardt *et al.*, 2008; Supplemental Figure S1B). Our results appear to be better explained by hypothesis 2.

Hypothesis 2 was proposed based on x-ray crystallography data by Burkhardt *et al.* (2008) showing that the N-peptide–binding mode and the "closed" syntaxin–binding mode take place simultaneously (Burkhardt *et al.*, 2008). In their biochemical binding experiments, WT syntaxin-1A binding to Munc18-1 prevented the formation of SNARE complex, whereas an N-peptide deletion mutant of syntaxin-1A still bound to Munc18-1 was more accessible to SNAP-25 and synaptobrevin-2, resulting in SNARE complex formation. This was due to the fact that the binding affinity between syntaxin-1A and Munc18-1 was reduced by the N-peptide deletion (Burkhardt *et al.*, 2008). Similarly, our binding experiments demonstrate that the binary interaction between syntaxin-1A and Munc18-1 is partially reduced by L8A mutation, whereas the interaction is barely detectable in the presence of L8A and L165A/E166A mutations together (Figures 8 and 9). Thus our results suggest that the N-peptide–binding mode and the "closed" conformation syntaxin-1–binding mode complement each other to ensure the tight interaction between syntaxin-1 and Munc18-1 (Figure 10). Our results are also consistent with the finding that syntaxin-1A either lacking N-peptide or bearing the LE mutation retains the structure of "closed" conformation when binding to Munc18-1 (Colbert *et al.*, 2013). Our results obtained with PC12 cells suggest that the physiological significance of the N-peptide binding is to ensure the trafficking of syntaxin-1 to the plasma membrane (Figures 3 and 4), presumably preventing the formation of ectopic SNARE complex (Medine *et al.*, 2007).

The degree to which syntaxin N-peptide plays a role in the interaction of monomeric syntaxin with Munc18 seems to be isoform

dependent; deletion of N-peptide in syntaxin-1 has little effect on its binding to Munc18-1, whereas similar deletion in syntaxin-4 dramatically reduces its binding to Munc18-3 (Christie *et al.*, 2012). Similarly, hydrophobic mutations in Munc18-1 or -2 almost completely abolish their binary binding to syntaxin-11 (Bin *et al.*, 2013), whereas the same mutations in Munc18-1 have little effect on its binding to syntaxin-1A (Malintan *et al.*, 2009). Therefore we argue that in the binding between neuronal syntaxin-1 and Munc18-1, the "closed" syntaxin–binding mode is so dominant that syntaxin-1 N-peptide becomes largely dispensable, but once this binding mode is compromised due to syntaxin-1 adopting the "open" conformation, N-peptide plays a crucial role in the binary interaction.

Hypothesis 1 was proposed based on assays measuring liposome fusion (Shen *et al.*, 2007, 2010), as well as fusion between large vesicles and giant membrane (Tareste *et al.*, 2008). In these assays, L8A mutation in syntaxin-1A abolished Munc18-1–mediated acceleration of SNARE-dependent fusion. To further test hypothesis 1, Zhou *et al.* (2013) assessed whether the phenotype of syntaxin-1B–knockdown neurons lacking syntaxin-1A could be rescued by expression of an N-peptide deletion (Δ8) mutant of syntaxin-1A. They demonstrated the inability of the mutant to rescue both miniature PSP frequency and evoked PSP amplitude. On the contrary, we did not see a strong reduction in the rescuing ability of N-terminal mutants (D3R, L8A) compared with the WT ("closed") conformation in both PC12 cells (Figure 3F) and *C. elegans* (Figures 6). We cannot explain the discrepancy between the two studies. However, another study showed that the hydrophobic pocket mutants of Munc18-1, which disrupt the binding to N-peptide of syntaxin-1, exhibit normal rescuing ability in synaptic exocytosis of Munc18-1–knockout neurons (Meijer *et al.*, 2012). This result suggests that the interaction between Munc18-1 hydrophobic pocket and N-peptide of syntaxin-1 is not essential for synaptic exocytosis. Of interest, Christie *et al.* (2012) obtained low-resolution structural data suggesting that the N-peptide binding mode and the closed binding mode are *not* compatible with each other, suggesting another hypothesis, hypothesis 3: N-peptide facilitates a transition from the "closed" to the "open" conformation of syntaxin-1 (Christie *et al.*, 2012). It is important to stress that our results do not exclude the critical importance of the N-peptide as a whole, which could perform functions other than securing the binary interaction of syntaxin-1 with Munc18-1.

Our discovery of a novel mutant form of Munc18-1 (Han *et al.*, 2013, 2014) transformed our understanding of how Munc18-1 functions downstream of vesicle docking. This mutant, which harbors mutations in domain-3a, completely loses its ability to rescue secretion. However, it effectively restores syntaxin-1 expression at the plasma membrane, as well as dense-core vesicle docking in Munc18-1/2 double-knockdown PC12 cells. Moreover, compared with the wild type or the hydrophobic pocket mutant, the novel mutant impairs binding to the SNARE complex (Han *et al.*, 2013). These results suggest that it is not the hydrophobic pocket of Munc18-1 but domain-3a that plays a crucial role in the postdocking stage of exocytosis through its interaction with the SNARE complex.

In conclusion, our results uncover the role of syntaxin-1 N- peptide, which becomes critical when the protein adopts an "open" conformation. Our findings also provide an important conceptual advance regarding the function of N-peptide of neuronal syntaxins. We propose that N-peptide of neuronal syntaxin-1 should be regarded as an integral component of the binary interaction with Munc18 rather than the essential motif to stimulate SNARE-mediated membrane fusion as previously suggested (Shen *et al.*, 2007). We speculate that the N-peptide is the conserved motif in all syntaxin isoforms that allows the binary interaction with Munc18s and that the evolutionary development of the "closed" conformation mode of neuronal syntaxins renders this motif less critical, specifically in neuronal exocytosis. In addition to the N-peptide, syntaxin-1 is composed of multiple domains that are also conserved: the Habc domain, the linker region, the H3 (SNARE) motif, and the transmembrane region. Future studies need to test the function(s) of each domain in order to elucidate the structural determinants of syntaxin-1 in mediating membrane fusion. We believe that the combination of our rescue assays of the stable syntaxin-1A/1B double-knockdown cells (D9) and *unc-64*–null *C. elegans* will serve as useful model systems to further analyze the structure/function relationship of syntaxin-1.

MATERIALS AND METHODS

General materials

Parental pLKO plasmid for lentivirus-mediated knockdown was purchased from Sigma-Aldrich (Oakville, Canada). Parental pLVX-IRES-puro plasmid for lentivirus-mediated expression of syntaxin-1A and 1B was purchased from Clontech Laboratories (Mountain View, CA). psPAX2 was purchased from Addgene (Cambridge, MA), and pMD.G was a kind gift from Tomoyuki Mashimo (University of Texas Southwestern Medical Center, Dallas, TX). We obtained monoclonal antibodies against syntaxin-1A and -1B (clone HPC-1; Barnstable *et al.*, 1985) from Sigma-Aldrich; Munc18-1 from BD Bioscience (Mississauga, Canada); SNAP-25 (clone SMI 81) from Covance (Princeton, NJ); GAPDH (clone 6C5) from Millipore (Billerica, MA); and polyclonal antibodies against syntaxin-2 from Synaptic Systems (Gottingen, Germany). Rabbit polyclonal syntaxin-1 antibody (I378) was a kind gift from Thomas Südhof (Howard Hughes Medical Institute/Stanford University, Stanford, CA).

Construction of syntaxin-1A/1B double-knockdown plasmids

To knock down rat syntaxin-1A and syntaxin-1B simultaneously, the 21-nucleotide sequence of CAGGTGGAAGAGATCCGGGGC (residues 106–126) in rat syntaxin-1A was targeted. This sequence is identical to that of syntaxin-1B, with the exception of one nucleotide (the underlined residue). CTCGAG was a hairpin turn to link sense and antisense sequence. Oligos of 58 base pairs containing sense and antisense of the target sequence were annealed and subcloned into the *Age*I-*Eco*RI sites of pLKO-puro, generating the syntaxin-1A/1B knockdown plasmid (pLKO-syntaxin-1KD). Inserted sequences were verified by DNA sequencing.

Isolation of stable syntaxin-1A/1B–knockdown PC12 cells

Wild-type PC12 cells were maintained in DMEM (Invitrogen, Carlsbad, CA) supplemented with 5% calf serum, 5% horse serum (both from HyClone, Logan, UT), penicillin (100 U/ml)/streptomycin (0.1 mg/ml; Sigma-Aldrich; Wang *et al.*, 2004, 2005; Li *et al.*, 2005, 2007; Fujita *et al.*, 2007; Arunachalam *et al.*, 2008), and, in some cases, 250 ng/ml amphotericin B (Sigma-Aldrich). Recombinant lentiviruses were generated by cotransfecting either pLKO-puro (control, 9 µg) or pLKO-syntaxin-1KD (9 µg) with two other plasmids (3 µg of pMD.G and 4.8 µg of psPAX2) into HEK-293FT (Invitrogen) cells using 40 µl of polyethylenimine (1.2 mg/ml, pH 7.2). The lentiviruses harvested from the HEK-293FT cells were applied to WT PC12 cells, which were subsequently selected with puromycin (2.5 µg/ml). A pool of heterogeneous cells that had survived in puromycin-containing medium over the period of 2 wk was

subjected to immunoblot analysis using anti–syntaxin-1 antibody. From the pool of heterogeneous cells, independent clones in which the silencing of syntaxin-1 was particularly strong were further isolated. These isolated cells were grown, frozen, and kept in a liquid nitrogen tank until use.

Quantification of protein expression levels

To quantify protein expression, a scanned image of immunoblot probed for a protein of interest was imported into ImageJ software (National Institutes of Health, Bethesda, MD). Using the gel analysis method, the intensity of individual bands was measured over the total intensity of all the bands in a selected area and expressed as a percentage of the total intensity. The identical immunoblot was also probed for a loading control such as GAPDH and analyzed by the foregoing method. Percentage values of the protein of interest were divided over those of the loading control to correct a problem of uneven loading. The ratio of control (wild-type pC12 cells) was set to 100, and the ratios of other samples were normalized to that of control.

Lentivirus-mediated syntaxin-1A and 1B expression constructs

The lentivirus-mediated expression constructs of wild-type and various mutants of syntaxin-1 were generated so that these proteins were stably expressed in the syntaxin-1A/1B double-knockdown cells. The parental expression plasmid was developed by replacing the puromycin resistance gene of pLVX-IRES-puro with a blasticidin resistance gene. SNMs (CAAGTCGAGGAAATTAGGG for 1A and CAAGTCGAGGAAATTAGGG for 1B; underlines indicate SNM) were introduced within the target sequence in the syntaxin-1A or 1B gene to protect the mRNA transcripts transcribed from the syntaxin-1 expression plasmid from being degraded by the anti–syntaxin-1 RNA interference machineries already induced within the syntaxin-1A/1B–knockdown cells. The digested syntaxin-1A (SNM) or syntaxin-1B (SNM) gene was subcloned into the *Eco*RI/*Xba*I site of the pLVX-IRES-blast plasmid. This syntaxin-1 expression plasmid was cotransfected with psPAX2 and pMD.G into HEK-293FT cells to generate recombinant lentiviruses that express syntaxin-1 variants. The syntaxin-1A/1B double- knockdown cells that were infected with lentiviruses expressing rescue proteins were selected with blasticidin (5 μg/ml).

Cell preparation for confocal immunofluorescence microscopy and image acquisition

Sterilized circular glass coverslips (0.25 mm in width, 1.8 cm in diameter) were placed in 2.2-cm wells within 12-well cell culture plates. The cover slips were then coated for 1 h with poly-D-lysine (0.1 mg/ml) at room temperature. Cells were allowed to adhere to the coverslips overnight and then differentiated on the coverslips for 3–4 d in DMEM supplemented with 100 ng/ml nerve growth factor (NGF; Sigma-Aldrich), 1% horse serum, 1% calf serum, and penicillin/streptomycin. The cells were washed with phosphate-buffered saline (PBS), fixed for 15 min with PBS containing 4% paraformaldehyde, and permeabilized with PBS containing 0.2% Triton X-100 and 0.3% bovine serum albumin (BSA) for 5 min. Nonspecific sites were blocked for 1 h at room temperature in PBS containing 0.3% BSA. Primary antibody directed against syntaxin1 (HPC-1 diluted 1:1000) was applied for 1 h. After three washes in blocking buffer, rhodamine red-X–conjugated anti-mouse antibodies (diluted 1:1000; from Jackson ImmunoResearch, West Grove, PA) were diluted in blocking buffer and applied for 1 h at room temperature. Samples were washed again three times in blocking buffer and then mounted using Fluoromount-G reagent (SouthernBiotech, Birmingham, AL). All images were acquired using a Zeiss laser confocal scanning microscope (LSM 510; Zeiss, Jena, Germany) with an oil immersion objective lens (63×).

Confocal image analysis

Images of NGF-differentiated PC12 cells were taken at an appropriate scale to allow the subsequent numerical analysis and imported into ImageJ software. To quantify localization of syntaxin-1, each cell in the images was divided into three regions: plasma membrane, intracellular compartments, and the nucleus. Regional divisions were attained by tracing the outline of the plasma membrane and the nucleus excluding neurites. Next the area and intensity of each region were measured; the area of a region was represented by the number of pixels within that region, and a regional intensity was the total of all pixel intensities within a region. To accommodate differences in cell sizes, regional intensity was divided by area of the respective region. Using area-normalized intensity, a localization ratio was calculated as follows: (area-normalized intensity of plasma membrane compartment)/(area-normalized intensity of intracellular compartment – area-normalized intensity of nucleus). The magnitude of the localization ratio represents the strength of the plasma membrane localization relative to intracellular regions for specific proteins analyzed.

[^{3}H]NA release assays from PC12 cells

PC12 cells were plated in 24-well plates; 3-4 d after plating, the cells were labeled with 0.5 μCi of [^{3}H]NA in the presence of 0.5 mM ascorbic acid for 12–16 h. The labeled PC12 cells were incubated with the fresh complete DMEM for 1–5 h to remove unincorporated [^{3}H]NA. The cells were washed once with physiological saline solution (PSS) containing 145 mM NaCl, 5.6 mM KCl, 2.2 mM $CaCl_2$, 0.5 mM $MgCl_2$, 5.6 mM glucose, and 15 mM 4-(2-hydroxyethyl)-1-piperazineethanesulfonic acid (HEPES), pH 7.4. NA secretion was stimulated with 200 μl of PSS or high-K^+ PSS (containing 81 mM NaCl and 70 mM KCl) at 37°C for 3 min and terminated by chilling on ice. Samples were centrifuged at 4°C for 3 min. Supernatants were removed for liquid scintillation counting, and the pellets were solubilized in 0.1% Triton X-100 to count intracellularly retained NA.

Maintenance of *C. elegans* strains

All strains were maintained at 22°C on NGM plates seeded with OP50, except EG4322 (*ttTi5605; unc-119(ed3)*), which was maintained at 15°C.

Generation of *C. elegans* worms expressing mammalian syntaxin-1A variants

pJH625, which contains the panneuronal promoter *PF25B3.3*, was used as a parental plasmid to express syntaxin-1A variants (Bouhours *et al.*, 2011). Each of the syntaxin-1A variants in pBluescript was digested with *Kpn*I and subcloned into a single *Kpn*I site in pJH625. A mixture of each pJH625-syntaxin-1A variant and a coinjection maker (pMyo3-RFP) was prepared such that the final concentration of each DNA was 50 ng/μl and injected into the gonads of young adult worms of the NM979 strain (genotype *unc-64(js115)/bli-5(e518) III*; Saifee *et al.*, 1998). At 3–4 d after the injection, the F1 generation, which is the progeny of the injected worms, was screened for red fluorescence, and only RFP-positive F1 worms were singled out.

Western blot analysis of *C. elegans* worms expressing mammalian syntaxin-1A proteins

Protein extract was prepared as described in Weimer *et al.* (2003). Briefly, worms were grown on large (10 cm) NGM plates. When the plates were full of worms with little OP50 left, worms were harvested and rinsed with water several times until the water was nearly clear. Washed worms were frozen at –80°C until use. Once ready for use, worms were quickly thawed under water and resuspended in 5–10 volumes of a solution containing 360 mM sucrose, 12 mM HEPES, and a protease inhibitor cocktail (1 µg/ml pepstatin A, 1 µg/ml leupeptin, 1 µg/ml aprotinin, 0.1 mM phenylmethylsulfonyl fluoride [PMSF]). The resuspended worms were then sonicated on ice four times with a 5-s burst at full power. The resulting lysate was centrifuged for 15 min to pellet the cuticle, nuclei, and other debris. After centrifugation, the supernatant was transferred to a clean microcentrifuge tube with an equal volume of 2× sample buffer. All of the subsequent steps were performed similarly to Western blot analysis using PC12 cell samples.

Locomotion assay

Locomotion assays were conducted by selecting *C. elegans* in the L4 stage and transferring them to a fresh OP50 NGM plate. The *C. elegans* animals were allowed to recover, and their movement was recorded for 10 min using an OMAX A3580U camera and the OMAX ToupView program over several days. Active locomotion was operationally defined as the movement of the tail end of the animal. The duration of active locomotion was obtained by manually observing and timing the *C. elegans* in each of the 10-min video recordings. The length of the *C. elegans* was calculated by tracing over the animal in Photoshop CS5 (Adobe, San Jose, CA) and converting the number of pixels in the trace to a length in millimeters. The most representative 60-s period of locomotion was selected from each of the recordings, and the speed of the animal in that duration was calculated by manually tracing the path traveled and then dividing this distance by 60 s.

GST pull-down assays probing interactions between recombinant GST-fused syntaxin-1A variants and Munc18-1 exogenously expressed in HEK298 cells

Rat syntaxin-1A cDNAs (1–264) encoding residues 1–264 WT and various mutants (L8A, LE, and LE+L8A) were subcloned into the *Eco*RI-*Hin*dIII site of pGex-KG (Dulubova *et al.*, 1999). The WT and mutant constructs were transformed into competent BL21 strain of *Escherichia coli*. The transformant colonies were grown in LB (lysogeny broth) on a small scale (5 ml) overnight at 37°C. On the next day, the bacteria were transferred to a larger culture container and grown in a bigger scale (50 ml) for 3 h at the same temperature. These bacteria were induced to generate recombinant proteins in the presence of 50 µM isopropyl-β-D-thiogalactopyranoside (IPTG) at 30°C for another 3 h. The bacteria were pelleted by centrifugation and resuspended in a PBS solution containing protease inhibitors (0.4 mM PMSF, 4 mM EDTA, 10 µg/ml leupeptin, and 10 µg/ml aprotinin). The resuspended bacteria were lysed by sonication for 15 s five times, and Triton X-100 was added to this lysate in a 1:100 dilution. The lysate was vortexed to mix up and chilled on ice for 5 min. This mixture was centrifuged, and the resulting supernatant was transferred to a microcentrifuge tube. Glutathione–Sepharose beads (Pierce Biotechnology, Waltham, MA) in 50% suspension with water was added to the supernatant to allow binding of proteins to the beads overnight. Meanwhile, HEK-293 cells, which exogenously expressed Munc18-1 after a transient transfection, were harvested and pelleted. These cells were washed with PBS containing 0.4 mM PMSF, and then 1 ml of KGlu binding buffer (20 mM HEPES, pH 7.2, 120 mM potassium glutamate, 20 mM potassium acetate, and 2 mM ethylene glycol tetraacetic acid containing 0.1% Triton X-100) was added to the cell pellet. After the pelleted cells were vortexed, they were homogenized using a $23^{1/2}$-gauge needle. The soluble part separated by centrifugation was incubated overnight with purified syntaxin-1 GST-fusion proteins immobilized on the glutathione beads. After incubation, Munc18-1–bound GST–syntaxin-1 proteins were washed five times with KGlu binding buffer and subjected to SDS–PAGE, followed by Ponceau S staining and immunoblotting.

GST pull-down assays probing interactions between recombinant GST-fused syntaxin-1A variants and His-tagged Munc18-1 WT

Recombinant GST-fused syntaxin-1A variants were purified as described. His_6-tagged Munc18-1 WT was generated by subcloning a 1.8-kb fragment of rat Munc18-1 WT (without stop codon) into the *Eco*RI/*Hin*dIII site of pET21a (Novagen, Madison, WI). This pET21a-Munc18-1 plasmid was transformed into BL21 (DE3) cells, and several transformant colonies were grown at 37°C until confluent. Recombinant Munc18-1 expression was induced by addition of 125 µM IPTG at 15°C overnight. On the next day, this culture was centrifuged at 3000 rpm for 10 min at 4°C using a JA-14 rotor (Beckman, Pasadena, CA). The resulting pellet was resuspended in a lysis buffer containing 20 mM Tris-HCl, 300 mM NaCl, 0.4% NP-40, 10 mM imidazole, 10 mM 2-mercaptoethanol, 1 mM PMSF, and 20 ng/ml DNase. Bacterial cell lysis was performed by applying a cell pressure of 1000 psi for 30 s three times using French pressure cell press (Thermo Scientific, Waltham, MA). The lysate was then centrifuged at 15,000 rpm for 30 min at 4°C using a JA-21 rotor. His_6-Munc18-1 supernatant was mixed with HisPur nickel-nitriloacetic acid resin (Thermo Scientific, Waltham, MA). The binding to beads was done for 2 h at 4°C. Subsequent washing was performed first by high-salt buffer (20 mM Tris-HCl, 500 mM NaCl, 20 mM imidazole, 10 mM 2-mercaptoethanol, 10% glycerol) followed by mid-salt buffer (same contents as high-salt buffer but with 300 mM NaCl instead). Then Munc18-1 proteins were eluted in an elution buffer (20 mM Tris-HCl, 150 mM NaCl, 250 mM imidazole, 10 mM 2-mercaptoethanol, 10% glycerol). Approximately12 µg of His_6-Munc18-1 proteins was added to 500 µl of KGlu binding buffer containing 10 µl of agarose beads with immobilized ~5 µg of GST–syntaxin-1A and incubated for 30 min at room temperature. The beads were washed five times with the binding buffer. After the washing, the total agarose beads were loaded onto SDS–PAGE gel and stained with Coomassie brilliant blue.

Purification of bacterially expressed proteins for isothermal titration calorimetry

His_6-tagged WT Munc18-1 was generated and purified as described. His_6-tagged cytosolic syntaxin-1A (1–265) variants (WT, L8A, LE, and LE+L8A) were generated by subcloning syntaxin fragments (without stop codon) into the *Eco*RI/*Hin*dIII site of pET21a (Novagen, Madison, WI). Purification of His_6-tagged syntaxin-1A proteins was as similar as that of His_6-tagged Munc18-1. However, 50 µM IPTG was used for induction of His_6-tagged syntaxin-1A proteins, and the concentration of NaCl in the lysis buffer was 150 mM instead of 300 mM. In addition, syntaxin-1A proteins were washed first by high-salt buffer and then by low-salt buffer (containing 150 mM NaCl). After elution, both the His_6-tagged Munc18-1 and syntaxin-1A proteins were further purified by gel filtration chromatography using HiLoad 26/60 Superdex 200 prep grad column in

ITC buffer (20 mM sodium phosphate buffer, 150 mM NaCl, and 1 mM dithiothreitol). Twenty fractions of 4-ml elutant were collected, and three or four fractions containing pure syntaxin-1A or Munc18-1 were combined and used for isothermal titration calorimetry within a few days.

Isothermal titration calorimetry analysis

ITC was carried out at 298 K using a MicroCal iTC200 (GE Healthcare, Chalfont St Giles, United Kingdom), with 26 × 2 µl injections of 100 µM syntaxin-1A–His_6 variants (WT, L8A, LE, and LE+L8A) into 5 µM Munc18-1-WT–His_6. Control ITC experiments were performed for each syntaxin-1A variant by injecting 100 µM syntaxin-1A into ITC buffer. Titration curves were generated using Origin software (OriginLab, Northampton, United Kingdom). Binding titration curves were subtracted with control titration curves to eliminate energy arising from intramolecular interactions between syntaxin-1A's. Thermodynamic parameters such as stoichiometry N, equilibrium association constant K_a ($=K_d^{-1}$), binding enthalpy ΔH, and binding entropy ΔS were obtained also from Origin software. The Gibbs free energy of binding ΔG was calculated from the relation $\Delta G = -RT \ln K_a$. Binding parameters were calculated as the average of three independent experiments ± SD.

Statistical analysis

For two-sample experiments, an independent t test was used, and a significance level of difference was considered if $p < 0.05$. For experiments with multiple samples, one-way analysis of variance was used, followed by post hoc tests such as Tukey's range test for a significance level of 0.05. All statistical analysis was done using Origin 7.

ACKNOWLEDGMENTS

We thank all of the members of the Zhen lab for invaluable contributions to the *C. elegans* work in this study and Michael Nonet (Washington University, St. Louis, MO) for his invaluable advice on the *C. elegans* work. We thank Josep Rizo (University of Texas Southwestern Medical Center, Dallas, TX) for advice on how to interpret our ITC data, as well as for allowing us to cite his group's unpublished data on analytical ultracentrifugation. We also thank F. A. Meunier and B. M. Collins (University of Queensland, Brisbane, Australia) for critically reading the manuscript and Thomas Südhof (Howard Hughes Medical Institute/Stanford University, Stanford, CA) for providing syntaxin-1 antibody (I378) and commenting on the manuscript. This research was supported by the Natural Sciences and Engineering Research Council of Canada (298461), the Heart and Stroke Foundation of Ontario (0171), and the Canadian Institute of Health Research (MOP-93665, 130573).

REFERENCES

Arunachalam L, Han L, Tassew N, He Y, Wang L, Xie L, Fujita Y, Kwan E, Davletov B, Monnier P, *et al.* (2008). Munc18-1 is critical for plasma membrane localization of syntaxin1 but not of SNAP-25 in PC12 cells. Mol Biol Cell 19, 722–734.

Barnstable C, Hofstein R, Akagawa K (1985). A marker of early amacrine cell development in rat retina. Brain Res 352, 286–290.

Bennett M, Calakos N, Scheller R (1992). Syntaxin: a synaptic protein implicated in docking of synaptic vesicles at presynaptic active zones. Science 257, 255–259.

Bin NR, Jung CH, Kim B, Chandrasegram P, Turlova E, Zhu D, Gaisano HY, Sun HS, Sugita S (2015). Chaperoning of closed syntaxin-3 through Lys46 and Glu59 in domain-1 of Munc18 is indispensable for mast cell exocytosis. J Cell Sci 128, 1946–1960.

Bin NR, Jung CH, Piggott C, Sugita S (2013). Crucial role of the hydrophobic pocket region of Munc18 protein in mast cell degranulation. Proc Natl Acad Sci USA 110, 4610–4615.

Bouhours M, Po MD, Gao S, Hung W, Li H, Georgiou J, Roder JC, Zhen M (2011). A co-operative regulation of neuronal excitability by UNC-7 innexin and NCA/NALCN leak channel. Mol Brain 4, 16.

Broadie K, Prokop A, Bellen H, O'Kane C, Schulze K, Sweeney S (1995). Syntaxin and synaptobrevin function downstream of vesicle docking in Drosophila. Neuron 15, 663–673.

Burgoyne RD, Morgan A (2007). Membrane trafficking: three steps to fusion. Curr Biol 17, R255–R258.

Burkhardt P, Hattendorf DA, Weis WI, Fasshauer D (2008). Munc18a controls SNARE assembly through its interaction with the syntaxin N-peptide. EMBO J 27, 923–933.

C. elegans Sequencing Consortium (1998). Genome sequence of the nematode C-elegans: a platform for investigating biology. Science 282, 2012–2018.

Christie MP, Whitten AE, King GJ, Hu SH, Jarrott RJ, Chen KE, Duff AP, Callow P, Collins BM, James DE, Martin JL (2012). Low-resolution solution structures of Munc18:Syntaxin protein complexes indicate an open binding mode driven by the Syntaxin N-peptide. Proc Natl Acad Sci USA 109, 9816–9821.

Colbert KN, Hattendorf DA, Weiss TM, Burkhardt P, Fasshauer D, Weis WI (2013). Syntaxin1a variants lacking an N-peptide or bearing the LE mutation bind to Munc18a in a closed conformation. Proc Natl Acad Sci USA 110, 12637–12642.

Darios F, Davletov B (2006). Omega-3 and omega-6 fatty acids stimulate cell membrane expansion by acting on syntaxin 3. Nature 440, 813–817.

Deák F, Xu Y, Chang WP, Dulubova I, Khvotchev M, Liu X, Südhof TC, Rizo J (2009). Munc18-1 binding to the neuronal SNARE complex controls synaptic vesicle priming. J Cell Biol 184, 751–764.

Dulubova I, Sugita S, Hill S, Hosaka M, Fernandez I, Südhof TC, Rizo J (1999). A conformational switch in syntaxin during exocytosis: role of munc18. EMBO J 18, 4372–4382.

Dulubova I, Yamaguchi T, Arac D, Li H, Huryeva I, Min SW, Rizo J, Sudhof TC (2003). Convergence and divergence in the mechanism of SNARE binding by Sec1/Munc18-like proteins. Proc Natl Acad Sci USA 100, 32–37.

Fujita Y, Xu A, Xie L, Arunachalam L, Chou T, Jiang T, Chiew S, Kourtesis J, Wang L, Gaisano H, Sugita S (2007). Ca2+-dependent activator protein for secretion 1 is critical for constitutive and regulated exocytosis but not for loading of transmitters into dense core vesicles. J Biol Chem 282, 21392–21403.

Fujiwara T, Mishima T, Kofuji T, Chiba T, Tanaka K, Yamamoto A, Akagawa K (2006). Analysis of knock-out mice to determine the role of HPC-1/syntaxin 1A in expressing synaptic plasticity. J Neurosci 26, 5767–5776.

Gengyo-Ando K, Kitayama H, Mukaida M, Ikawa Y (1996). A murine neural-specific homolog corrects cholinergic defects in Caenorhabditis elegans unc-18 mutants. J Neurosci 16, 6695–6702.

Gerber S, Rah J, Min S, Liu X, de Wit H, Dulubova I, Meyer A, Rizo J, Arancillo M, Hammer R, *et al.* (2008). Conformational switch of syntaxin-1 controls synaptic vesicle fusion. Science 321, 1507–1510.

Han GA, Bin NR, Kang SY, Han L, Sugita S (2013). Domain 3a of Munc18-1 plays a crucial role at the priming stage of exocytosis. J Cell Sci 126, 2361–2371.

Han GA, Malintan NT, Collins BM, Meunier FA, Sugita S (2010). Munc18-1 as a key regulator of neurosecretion. J Neurochem 115, 1–10.

Han GA, Malintan NT, Saw NM, Li L, Han L, Meunier FA, Collins BM, Sugita S (2011). Munc18-1 domain-1 controls vesicle docking and secretion by interacting with syntaxin-1 and chaperoning it to the plasma membrane. Mol Biol Cell 22, 4134–4149.

Han GA, Park S, Bin NR, Jung CH, Kim B, Chandrasegaram P, Matsuda M, Riadi I, Han L, Sugita S (2014). A pivotal role for Pro335 in balancing the dual functions of Munc18-1 domain-3a in regulated exocytosis. J Biol Chem 289, 33617–33628.

Han L, Jiang T, Han G, Malintan N, Xie L, Wang L, Tse F, Gaisano H, Collins B, Meunier F, Sugita S (2009). Rescue of Munc18-1 and -2 double knockdown reveals the essential functions of interaction between Munc18 and closed syntaxin in PC12 cells. Mol Biol Cell 20, 4962–4975.

Harrison SD, Broadie K, van de Goor J, Rubin GM (1994). Mutations in the Drosophila Rop gene suggest a function in general secretion and synaptic transmission. Neuron 13, 555–566.

Hosono R, Hekimi S, Kamiya Y, Sassa T, Murakami S, Nishiwaki K, Miwa J, Taketo A, Kodaira KI (1992). The unc-18 gene encodes a novel protein affecting the kinetics of acetylcholine metabolism in the nematode Caenorhabditis elegans. J Neurochem 58, 1517–1525.

Hu SH, Latham CF, Gee CL, James DE, Martin JL (2007). Structure of the Munc18c/Syntaxin4 N-peptide complex defines universal features of the N-peptide binding mode of Sec1/Munc18 proteins. Proc Natl Acad Sci USA 104, 8773–8778.

Jahn R (2004). Principles of exocytosis and membrane fusion. Ann NY Acad Sci 1014, 170–178.
Khvotchev M, Dulubova I, Sun J, Dai H, Rizo J, Südhof TC (2007). Dual modes of Munc18-1/SNARE interactions are coupled by functionally critical binding to syntaxin-1 N terminus. J Neurosci 27, 12147–12155.
Kofuji T, Fujiwara T, Sanada M, Mishima T, Akagawa K (2014). HPC-1/syntaxin 1A and syntaxin 1B play distinct roles in neuronal survival. J Neurochem 130, 514–525.
Lerman JC, Robblee J, Fairman R, Hughson FM (2000). Structural analysis of the neuronal SNARE protein syntaxin-1A. Biochemistry 39, 8470–8479.
Li G, Han L, Chou T, Fujita Y, Arunachalam L, Xu A, Wong A, Chiew S, Wan Q, Wang L, Sugita S (2007). RalA and RalB function as the critical GTP sensors for GTP-dependent exocytosis. J Neurosci 27, 190–202.
Li G, Lee D, Wang L, Khvotchev M, Chiew S, Arunachalam L, Collins T, Feng Z, Sugita S (2005). N-terminal insertion and C-terminal ankyrin-like repeats of alpha-latrotoxin are critical for Ca2+-dependent exocytosis. J Neurosci 25, 10188–10197.
Liu Y, Schirra C, Edelmann L, Matti U, Rhee J, Hof D, Bruns D, Brose N, Rieger H, Stevens D, Rettig J (2010). Two distinct secretory vesicle-priming steps in adrenal chromaffin cells. J Cell Biol 190, 1067–1077.
Malintan N, Nguyen T, Han L, Latham C, Osborne S, Wen P, Lim S, Sugita S, Collins B, Meunier F (2009). Abrogating Munc18-1-SNARE complex interaction has limited impact on exocytosis in PC12 cells. J Biol Chem 284, 21637–21646.
Medine CN, Rickman C, Chamberlain LH, Duncan RR (2007). Munc18-1 prevents the formation of ectopic SNARE complexes in living cells. J Cell Sci 120, 4407–4415.
Meijer M, Burkhardt P, de Wit H, Toonen RF, Fasshauer D, Verhage M (2012). Munc18-1 mutations that strongly impair SNARE-complex binding support normal synaptic transmission. EMBO J 31, 2156–2168.
Mishima T, Fujiwara T, Kofuji T, Akagawa K (2012). Impairment of catecholamine systems during induction of long-term potentiation at hippocampal CA1 synapses in HPC-1/syntaxin 1A knock-out mice. J Neurosci 32, 381–389.
Mishima T, Fujiwara T, Sanada M, Kofuji T, Kanai-Azuma M, Akagawa K (2014). Syntaxin 1B, but not Syntaxin 1A, is necessary for the regulation of synaptic vesicle exocytosis and of the readily releasable pool at central synapses. PLoS One 9, e90004.
Misura KM, Scheller RH, Weis WI (2000). Three-dimensional structure of the neuronal-Sec1-syntaxin 1a complex. Nature 404, 355–362.
Nonet ML, Saifee O, Zhao H, Rand JB, Wei L (1998). Synaptic transmission deficits in Caenorhabditis elegans synaptobrevin mutants. J Neurosci 18, 70–80.
Ogawa H, Harada S, Sassa T, Yamamoto H, Hosono R (1998). Functional properties of the unc-64 gene encoding a Caenorhabditis elegans syntaxin. J Biol Chem 273, 2192–2198.
Peters JM, Walsh MJ, Franke WW (1990). An abundant and ubiquitous homo-oligomeric ring-shaped ATPase particle related to the putative vesicle fusion proteins Sec18p and NSF. EMBO J 9, 1757–1767.
Rathore SS, Bend EG, Yu H, Hammarlund M, Jorgensen EM, Shen J (2010). Syntaxin N-terminal peptide motif is an initiation factor for the assembly of the SNARE-Sec1/Munc18 membrane fusion complex. Proc Natl Acad Sci USA 107, 22399–22406.
Richmond JE, Weimer RM, Jorgensen EM (2001). An open form of syntaxin bypasses the requirement for UNC-13 in vesicle priming. Nature 412, 338–341.
Saifee O, Wei L, Nonet ML (1998). The Caenorhabditis elegans unc-64 locus encodes a syntaxin that interacts genetically with synaptobrevin. Mol Biol Cell 9, 1235–1252.
Schoch S, Deák F, Königstorfer A, Mozhayeva M, Sara Y, Südhof T, Kavalali E (2001). SNARE function analyzed in synaptobrevin/VAMP knockout mice. Science 294, 1117–1122.
Schulze K, Broadie K, Perin M, Bellen H (1995). Genetic and electrophysiological studies of Drosophila syntaxin-1A demonstrate its role in non-neuronal secretion and neurotransmission. Cell 80, 311–320.
Sharma N, Low SH, Misra S, Pallavi B, Weimbs T (2006). Apical targeting of syntaxin 3 is essential for epithelial cell polarity. J Cell Biol 173, 937–948.
Shen J, Rathore S, Khandan L, Rothman J (2010). SNARE bundle and syntaxin N-peptide constitute a minimal complement for Munc18-1 activation of membrane fusion. J Cell Biol 190, 55–63.
Shen J, Tareste DC, Paumet F, Rothman JE, Melia TJ (2007). Selective activation of cognate SNAREpins by Sec1/Munc18 proteins. Cell 128, 183–195.
Söllner T, Bennett M, Whiteheart S, Scheller R, Rothman J (1993). A protein assembly-disassembly pathway in vitro that may correspond to sequential steps of synaptic vesicle docking, activation, and fusion. Cell 75, 409–418.
Stewart S, Dykxhoorn D, Palliser D, Mizuno H, Yu E, An D, Sabatini D, Chen I, Hahn W, Sharp P, *et al*. (2003). Lentivirus-delivered stable gene silencing by RNAi in primary cells. RNA 9, 493–501.
Südhof TC, Rothman JE (2009). Membrane fusion: grappling with SNARE and SM proteins. Science 323, 474–477.
Tareste D, Shen J, Melia TJ, Rothman JE (2008). SNAREpin/Munc18 promotes adhesion and fusion of large vesicles to giant membranes. Proc Natl Acad Sci USA 105, 2380–2385.
Verhage M, Maia A, Plomp J, Brussaard A, Heeroma J, Vermeer H, Toonen R, Hammer R, van den Berg T, Missler M, *et al*. (2000). Synaptic assembly of the brain in the absence of neurotransmitter secretion. Science 287, 864–869.
Wang L, Li G, Sugita S (2004). RalA-exocyst interaction mediates GTP-dependent exocytosis. J Biol Chem 279, 19875–19881.
Wang L, Li G, Sugita S (2005). A central kinase domain of type I phosphatidylinositol phosphate kinases is sufficient to prime exocytosis: isoform specificity and its underlying mechanism. J Biol Chem 280, 16522–16527.
Washbourne P, Thompson P, Carta M, Costa E, Mathews J, Lopez-Benditó G, Molnár Z, Becher M, Valenzuela C, Partridge L, Wilson M (2002). Genetic ablation of the t-SNARE SNAP-25 distinguishes mechanisms of neuroexocytosis. Nat Neurosci 5, 19–26.
Weimer RM, Richmond JE, Davis WS, Hadwiger G, Nonet ML, Jorgensen EM (2003). Defects in synaptic vesicle docking in unc-18 mutants. Nat Neurosci 6, 1023–1030.
Zhou P, Pang ZP, Yang X, Zhang Y, Rosenmund C, Bacaj T, Südhof TC (2013). Syntaxin-1 N-peptide and H(abc)-domain perform distinct essential functions in synaptic vesicle fusion. EMBO J 32, 159–171.
Zhu D, Koo E, Kwan E, Kang Y, Park S, Xie H, Sugita S, Gaisano HY (2013). Syntaxin-3 regulates newcomer insulin granule exocytosis and compound fusion in pancreatic beta cells. Diabetologia 56, 359–369.

Supplemental Materials

Molecular Biology of the Cell

Park et al.

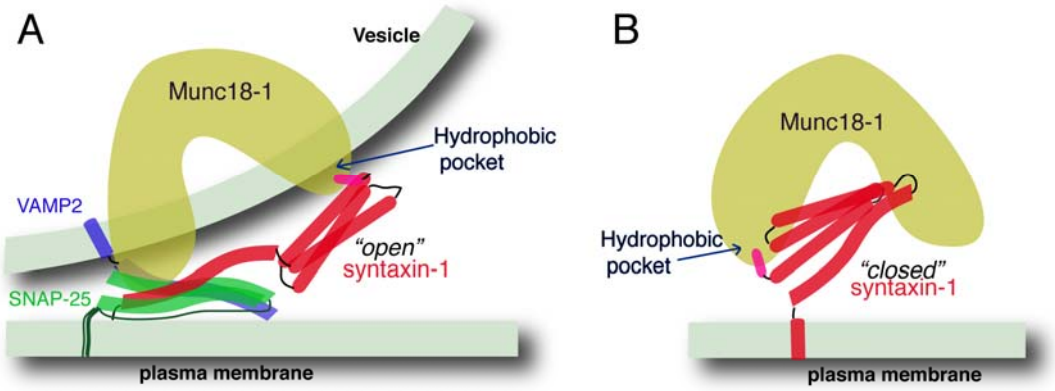

The N-peptide is required for Munc18-1 to interact with the SNARE complex and accelerate SNARE-mediated membrane fusion.

The N-peptide and the remaining regions of syntaxin-1 cooperate for high affinity binding to Munc18-1.

Figure S1.
Park et al.

Supplemental Figure S1. Two different models regarding the role of syntaxin-1 N-peptide. (A) It is essential for Munc18-1 mediated priming of SNARE-dependent fusion by allowing the binding of Munc18-1 to the SNARE complex (Burgoyne and Morgan, 2007; Südhof and Rothman, 2009). (B) It secures the Munc18-1/“closed” syntaxin-1 complex to block the formation of ectopic SNARE complexes (Burkhardt *et al.*, 2008).

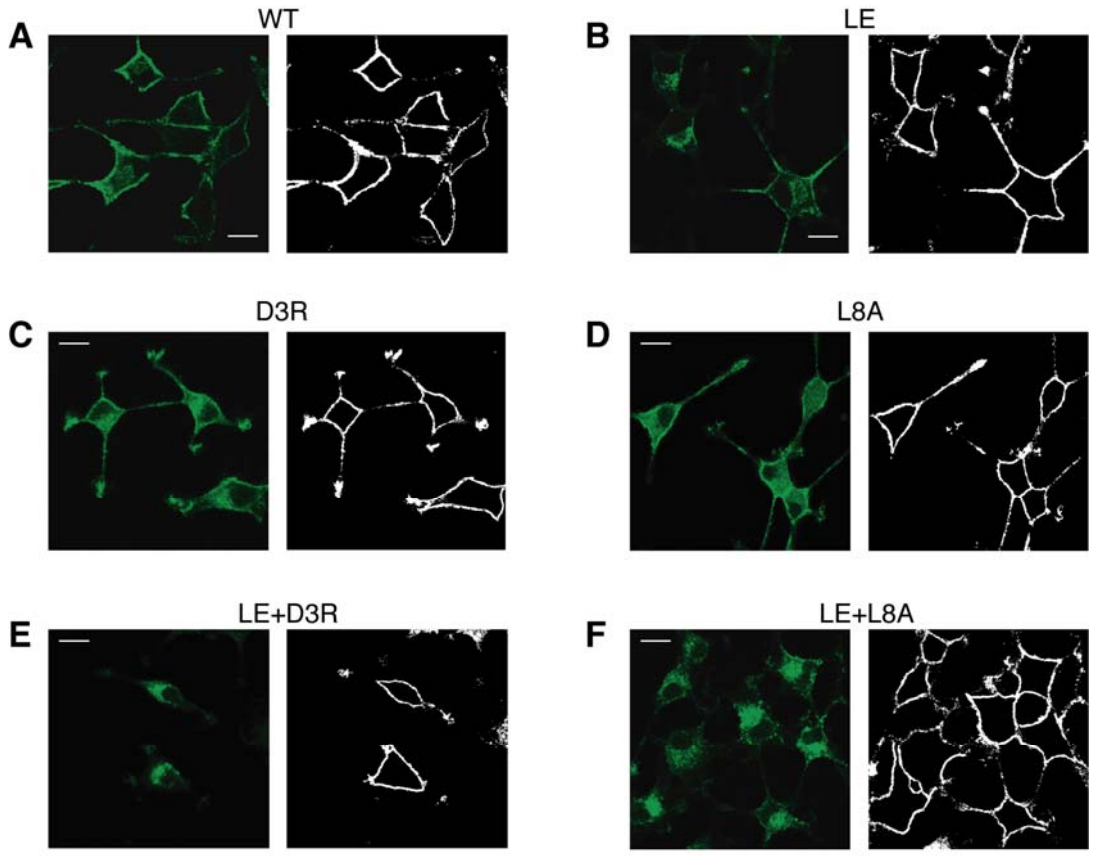

Figure S2.
Park et al.

Supplemental Figure S2. Confocal images of syntaxin-1 DKD cells expressing various forms of syntaxin-1A. (A-F) (Left) Confocal images are identical to those in Figure 2. (Right) Outlines of the cells shown in the confocal images are drawn in white.

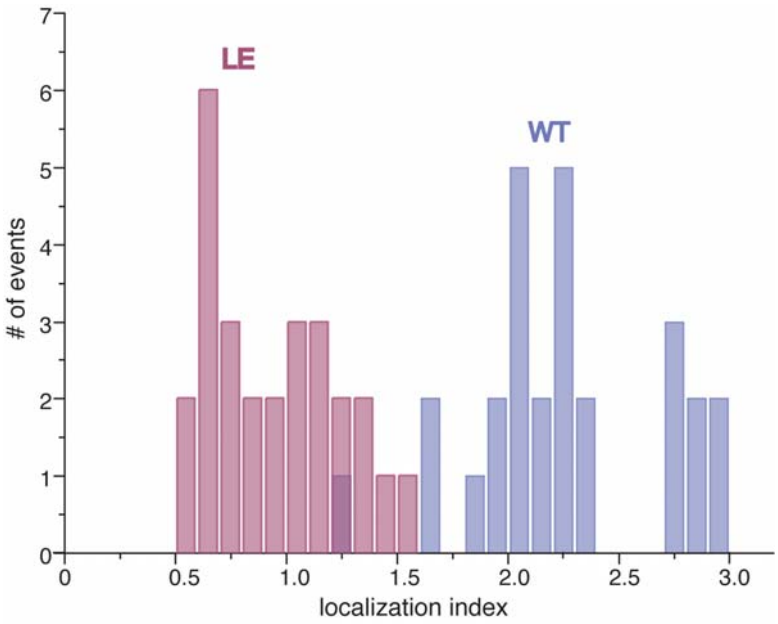

Figure S3.
Park et al.

Supplemental Figure S3. The distribution histogram of localization index values for D9 cells rescued by WT and LE "open" mutant.

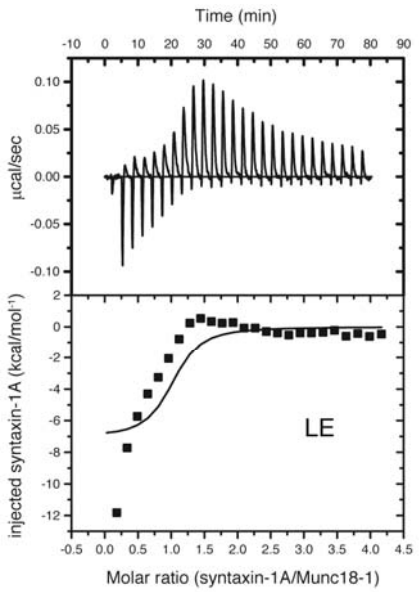

Figure S4.
Park et al.

Supplemental Figure S4. Simulated isothermal calorimetry analysis of binding between His6-tagged syntaxin-1A (1-265) LE "open" mutant and His6-tagged Munc18-1. Top panel illustrates representative raw ITC data and bottom panel illustrates integrated and normalized ITC data for the binding when fitted to N=1.